J. Math. Biol. (1999) 38: 377–421

Journal of Mathematical Biology

A mathematical analysis of Jones's site model for spruce budworm infestations

D. C. Hassell[1,2], D. J. Allwright[1], A. C. Fowler[1]

[1] Mathematical Institute, Oxford University, 24-29 St Giles', Oxford OX1 3LB, UK. e-mail: fowler@maths.ox.ac.uk
[2] Present address: Hadley Centre, Meteorological Office, London Road, Bracknell, Berkshire RG12 2SY, UK

Received: 7 July 1997 / Revised version: 20 July 1998

Abstract. The budworm site model of Jones (1979) is a complicated representation of the interaction between the spruce budworm and the forests of Northeastern Canada, which describes the way in which the budworm population undergoes periodic outbreaks, which lead to severe defoliation and widespread tree mortality. We show how this model can be systematically simplified without gainsaying the essential description of the budworm/forest interaction. The main simplification is the collapse of the year to year age structure to allow for three classes of young, mature, and old trees; we then obtain a reduced set of six difference equations for the six variables: larval population, new and old foliage, and the three age classes. Further analysis and reduction of the model is then possible on the basis of formal asymptotic limits, and we analyse a reduced model consisting of three difference equations for larvae, (old) foliage, and the area fraction of mature trees. In practice, the latter variable is inessential to the mechanism of oscillation, which can be understood via the slow cycling of the foliage variable round a hysteresis loop of quasi-steady states, mediated by the varying larval population as control parameter.

Key words: Spruce budworm – Difference equations – Site model – Hysteresis – Oscillations

1. Introduction

The interaction between the spruce budworm moth (*Choristoneura fumiferana*) and the forests of North America provides an excellent

pedagogical example of the application of mathematical modelling to a dynamical ecological system. Spruce budworm infestations occur at regular intervals in the forests of New Brunswick, with a period on the order of 35 years. These outbreaks cause severe damage, and are of consequent economic importance. An extensive field study (the Green River project) in the 1950s led to the publication of a monograph (Morris 1963) which gave a detailed description of the dynamics of the interaction between the budworm (specifically, in the larval stage) and the trees whose foliage it devours, chiefly spruce and balsam fir. A more colloquial account is given by Belyea et al. (1975). Following this, a detailed simulation model was developed by Jones (1979), and called here the budworm site model. (In its entirety, the simulation allows the evolution of the key variables at a large number of different sites, with moth migration facilitating an effective larval transport between sites.) The key variables are the larval population, the quantities of new (first year) and old foliage, and the fractional area occupied by 75 different age classes of trees (separated by a year's gap in age, essentially). In its operation, the model updates these key variables year by year in each of 393 sites, thus giving $78 \times 393 = 30{,}654$ difference equations for the spatially distributed key variables.

For the applied mathematician, a major question is whether any useful simplification of the site model can be made: even if we restrict ourselves to a single site, 78 variables is far too many to admit any analytical insight. The classic paper which carries out such a simplification is that of Ludwig, Jones and Holling (1978), who devise a much simpler model describing the behaviour of three key variables, which may be thought of as larval density, foliage density, and (mature) tree density. Their model uses differential equations, and is phenomenological insofar as it treats the key effects (predation, foliage consumption, etc.) in a plausible descriptive way rather than aiming to give a precise reduction of the original site model. The incorporation of spatial variation to this model is presumably best done by incorporating larval diffusion (representing adult moth migration) as Ludwig et al. (1979) did, notwithstanding the fact that adult moths can be transported by prevailing winds by up to 25 miles in a single night.

Our aim in this paper is to derive a reduced form of the original Jones budworm site model. Indeed, we shall show that the dynamics of the model can be usefully compressed to that of three, or even two, first order difference equations, but that the structure of these is very different to the Ludwig–Jones–Holling (LJH) model. Nevertheless, regular outbreaks occur, and indeed, the character of the oscillations (cycling round a hysteresis loop by the slow variation of a control variable) is similar.

The Jones model is perhaps the most prominent model of the budworm/forest system. Other related papers are those by Stedinger (1984), McNamee et al. (1981) and Régnière and You (1991), while Horowitz and Ioinovici (1985) analyse the LJH model as a feedback control system. However, the model has been subjected to criticism by Royama (1984, 1992), who contends that some of its implications are inconsistent with some of the Green River data. The principal components in the Jones simulation model, and also in the LJH model, are the budworm larval density (l), the foliage density (g), and the mature tree density (χ). (The equivalents of these variables in the LJH model are B, E, and S.) Essentially, growth and mortality of the larvae are controlled by the extent of defoliation, with predation by birds also being of importance. Thus in the Jones or LJH model, budworm decline follows defoliation. In contradistinction, Royama (1992) asserts that neither defoliation nor tree mortality can be a cause of larval decline, because budworm decline in different plots of the Green River watershed was independent of defoliation, and also the decline in Cape Breton, Nova Scotia, preceded tree mortality. Royama favours a population oscillation of predator prey type between the budworm (prey) and various host parasitoids, rather than the decimation due to competition envisaged in the Jones model. We shall return to this issue in the discussion.

In Sect. 2, we give a complete description of the budworm site model, and write down the governing equations in dimensionless form. Section 3 concerns the reduction of the model, primarily by collapsing the age structure to three classes: young, mature, and old. We then analyse the reduced (six variable) model further in Sect. 4, indicating how the larval, foliage and tree age subsystems behave separately in healthy forest. To analyse the model further, we use two formal asymptotic limits which reduce the model to one for three variables. This (and a further two-variable model) allows outbreaks to occur, and we analyse the conditions which determine outbreaks.

Finally, in Sect. 5 we show how the inclusion of small regeneration terms (via growth of seedlings) allows regular oscillations to occur, in a manner conceptually similar to that governing the Ludwig et al. (1978) oscillations. The conclusions in Sect. 6 give a colloquial explanation of our findings, as well as providing further discussion of the relative merits of the Jones and Royama models.

2. The budworm site model

In his simulation model of spruce budworm infestations of the forests of New Brunswick, Jones (1979) divided the province into 393 *sites*, of

area 65.8 square miles each. Each site was described by the *budworm site model*, and the interaction between sites was effected by the dispersal of adult moths between sites. In this paper we are concerned with the dynamics of the site model alone, and to that end we will ignore the dispersal and influx terms which are present in the full simulation model; for completeness, though, these are included in the present section.

The model has three principal constituents, which are budworm larvae, foliage, and tree density, and since the budworm cycles through its lifespan once a year, the model takes the form of difference equations which relate the values of the variables in succeeding years. These are complicated by virtue of the fact that larval development (through six *instars* – the stages between successive moults), foliage age, and tree age are all included in the model. This renders the site model fearsomely complicated. In order to present the model, we describe it verbally in this section, and give the governing relations in dimensional form. At the end of each section, however, the relevant equation is then summarised in a *dimensionless* form. For recourse to the original variables, reference must be made to Jones's (1979) original paper, although for ease of reference, we compare our notation with that of Jones in Appendix A, and give a definition of the dimensionless parameters in Appendix B.

2.1. Model variables

We define $l(t)$ to be the large larval population (instars III–VI) in year t, which consists of those small larvae (instars I–II) which survive. The larvae consume foliage, which is divided into new (this year's) foliage $f(t)$ (which the larvae prefer) and old foliage $g(t)$. Finally, the tree population is divided into 75 age classes which are associated with the age of the trees. Specifically, classes 1 to 21 represent immature upper storey trees which are not susceptible to budworm attack, and classes 74 and 75 represent old trees (older than about 95 years). Other than these, trees advance from age class i to $i + 1$ each year, and the relevant variable is $T_i(t)$, which measures the fraction of land in the site occupied by trees of age class i. The site model therefore describes the year to year evolution of the 78 variables l, f, g and T_i, $i = 1, \ldots, 75$. We now describe the evolution of these variables in turn. Unless stated otherwise, all variables are evaluated in year t.

2.2. Budworm survival

The larval density l is measured in units of ind tsf^{-1}, (individuals per ten square feet of susceptible branch surface area), and we have

$l(t+1) = Ss$, where S is the survival proportion of small larvae, and s is the small larvae density (ind tsf^{-1}). Small larvae need to find foliage in two dispersals (one in autumn, one in spring) in order to survive, and therefore we have $S = \Theta_0 IB$, where Θ_0 is a scaling factor (associated with natural mortality), I is the probability of two successful searches for foliage, and B is a relative measure of susceptible branch surface area, defined by $B = b/b_0$, where b = total branch surface area (tsf acre^{-1}), and b_0 (tsf acre^{-1}) is an average total for healthy forest. We take $I = G_1 G_2$, where

$$G_1 = \frac{w}{h_0}\left(\Theta_1 - \frac{w}{h_0}\right),$$
$$G_2 = \frac{z}{h_0}\left(\Theta_1 - \frac{z}{h_0}\right), \tag{2.1}$$

w and z (fu tsf^{-1}) being total foliage density in autumn and spring respectively, h_0 is the total foliage density at the start of the year in the absence of budworm, Θ_1 is a constant. The unit of foliage (fu) is simply defined as the quantity of foliage on ten square feet of susceptible branch surface area in the absence of budworm. Jones (1979) used foliage units for both quantity and density, but here fu refers always to a quantity.

The small larval density immediately after hatching (in autumn) depends on the number of eggs surviving: $s = Ee$, where E is the surviving proportion, e is the egg density on susceptible foliage (i.e. foliage on trees not about to die), which is given by $e = G_1 \bar{a}$, where G_1 is the same as in $(2.1)_1$, and is the probability of a successful search by adult female moths for a suitable oviposition site. The point is that survival of egg through hatching to instar II level in spring relies on G_1 twice: hatching of the egg, and then subsequent survival through instar I. $\bar{a}$ is the potential egg density (ind tsf^{-1}), and is due both to those generated on site, and those which migrate (we think of eggs migrating through the dispersal of adult moths). Here we ignore the latter, and identify $\bar{a} = d$, the density of eggs generated on site. This is given by $d = AR\bar{v}a$, where A is the fraction of females surviving to lay eggs (a constant), R is the proportion of adults which are female, $\bar{v}$ is the number of eggs carried by an adult female moth (a measure of fecundity), and a is the density of adult moths (ind tsf^{-1}).

The proportion of females is taken to be a function of pupal survival, $R = \Lambda_3 + \Lambda_4 P$, where P is the fraction of pupae surviving to adulthood, and Λ_3, Λ_4 are constants. The fecundity is assumed to be determined by the amount of food consumed by large larvae. These feeding levels affect the pupal case size which has been shown to

have a linear relationship with adult fertility (Morris 1963). Large larvae consume different but related amounts of old and new foliage. The resulting pupal weight is represented by the quantity $M = \Sigma_0 X + \Sigma_1 Y - \Sigma_2$, where X and Y are the proportions of new and old foliage consumed per large larva as a fraction of the maximum desired amount of all foliage, and then fecundity is taken as $\bar{v} = \Sigma_3 M^{1/3} - \Sigma_4$; Σ_i are constants. We also assume $\bar{v} \geqq v_0$ (a constant), insofar as too low levels of pupal feeding will not allow them to survive.

The density of adults on site (before dispersal) is $a = Pp$, where the pupal density $p = Ll$, and L is a survival factor (the proportion of large larvae surviving to pupation). The proportion of pupae which survive is $P = \Upsilon_0 + \Upsilon_1 L$, and is related to larval survival because the mortality risks are related; Υ_0 and Υ_1 are constants.

The site model allows for four factors affecting larval survival: food limitation, weather, parasitism, and avian predation. The surviving proportion of larvae to instar VI due to the first three factors is given by $K = \Phi_0 \bar{X} W Z$, where Φ_0 is a constant, $\bar{X}$ is the proportion surviving parasitism, Z is the total foliage consumed per large larva as a fraction of the maximum possible consumption, and W is a weather factor, which in practice acts in the model as a stochastic input. The parasitism survival rate depends on larval density, thus

$$\bar{X} = 1 - \Phi_1 \exp(-\Phi_2 l), \tag{2.2}$$

and Z is described further below. The density of large larvae surviving at the beginning of instar VI is then $k = Kl$.

Predation is due to three classes of birds (Morris 1963) and is assumed to affect only instar VI larvae (Mook 1963). Birds only search foliage covered branches, so the effective larval density for predation is $\bar{k} = kh_0/h$, where h (fu tsf^{-1}) is the total density of foliage at the start of the year. The proportion of larvae removed at a visit by class j birds is supposed to be

$$P_j = \frac{A_j}{e^{-C_j k} + B_j \bar{k}}, \tag{2.3}$$

where A_j, B_j, C_j are predation coefficients, and the total response is $Q = \sum_j P_j$. Associated with the assumption of a negative binomial distribution of the number of visits (Griffith and Holling 1969), Jones takes the survival rate $\bar{P}$ from avian predation as

$$\bar{P} = \left(1 + \frac{Q}{\Phi_3 B A_0}\right)^{-A_0}, \tag{2.4}$$

with Φ_3 a scaling factor, and A_0 a 'clumping' factor which describes the way in which attacks are distributed on the site (May 1978). The total survival factor of large larvae to pupation is thus $L = K\bar{P}$.

2.3. *Foliage consumption and renewal*

The ratios of consumption of new (q) and old (r) foliage are given (in fu ind^{-1} y^{-1}) by

$$q = \frac{f}{l\Delta t}\left[1 - \exp\left(-\frac{c_0 l\Delta t}{f}\right)\right],$$
$$r = \frac{g}{l\Delta t}\left[1 - \exp\left(-\frac{(c_0 - q)\, l\Delta t}{f}\right)\right], \tag{2.5}$$

where c_0 is the maximum rate of consumption (fu ind^{-1} y^{-1}), f and g are new and old foliage densities (fu tsf^{-1}) at the beginning of the year, $\Delta t = 1$ year, and (2.5) recognises that new foliage is preferred: c_0 is the demand for q, while $c_0 - q$ is therefore the demand for r. The relative measures X, Y, Z defined above are then given by $X = q/c_0$, $Y = r/c_0$, $Z = X + Y$.

The total defoliations of new and old foliage are given by $\bar{q} = ql\Delta t$, $\bar{r} = rl\Delta t$, and then the new and old foliage densities after defoliation are $u = f - \bar{q}$, $v = g - \bar{r}$, and the total (defoliated) foliage density is $w = u + v$. If x and y denote the new and old foliage densities after tree mortality is taken into account, then we can put

$$u = Jx + (1 - J)\bar{x},$$
$$v = Jy + (1 - J)\bar{y}, \tag{2.6}$$

where J (defined later) is the proportion of susceptible trees that survive to year $t + 1$, and we assume the new and old foliage densities on trees which die to be $\bar{x} = \Gamma_0 x$, $\bar{y} = \Gamma_0 y$, with $0 < \Gamma_0 < 1$. From (2.6), we determine x and y, and then the total foliage density after tree mortality is $z = x + y$.

Spring foliage production occurs as a result of photosynthetic assimilation, and this is assumed to occur at a rate $\bar{A} = z/h_0$; the production of new foliage is then $m = \bar{A}f_0$, where f_0 is the density of new foliage produced in the absence of budworm. The proportion of new foliage which survives tree mortality to become old foliage in year $t + 1$ is $W_1 = 1 - \Omega_0 x$, with Ω_0 a constant. The old foliage survival rate is taken as $W_2 = (\Omega_2 - \Omega_1 \bar{A})\bar{A}$, with Ω_i being constants, so that the old foliage density carried into year $t + 1$ is $n = W_1 x + W_2 y$. In

terms of these quantities, the foliage update equations are

$$f(t+1) = \frac{cf_0 + bm}{c+b}, \qquad g(t+1) = \frac{cg_0 + bn}{c+b}, \tag{2.7}$$

where b is the branch surface area (tsf acre^{-1}) of all susceptible trees surviving to year $t+1$, and c is that of those becoming susceptible for the first time in year $t+1$ (these are defined below). The total updated foliage density is then $h = f + g$.

2.4. Tree mortality

The effect of defoliation is to stress the tree, and this is measured by the stress $T = \Psi_2(1-U)^2$, with Ψ_2 a constant, and $U = v/g_0$ is the (relative) amount of old foliage present after defoliation (if $U > 1$, we take $T = 0$). The trees are divided into 75 age classes, labelled by $i = 1, 2, \ldots, 75$, and then T_i is the fraction of host land occupied by trees of age class i, so that $\sum_{i=1}^{75} T_i = 1$. Trees in age classes 1 to 21 are non-susceptible, while those in classes 22 to 75 are susceptible to attack. The susceptible land fraction is then $D = \sum_{i=22}^{75} T_i$. We define the mortality fraction of trees in age class i dying in year t as $M_i = \mu_i T$, where μ_i is a (given) age specific mortality factor (and $\mu_i = 0$ for $i < 22$). It follows that $C = \sum_{i=22}^{75} T_i M_i$ is the land fraction cleared of trees, and $J = 1 - (C/D)$ is the proportion of susceptible trees surviving defoliation. After mortality, it is assumed that regeneration occurs with trees of age class 1. Natural tree mortality affects classes 74 and 75 at a rate Ψ_3, leading to a land fraction loss of $\bar{H} = \Psi_3(U_{74} + U_{75})$, where, for each i, $U_i = T_i(1 - M_i)$ is the fraction of trees in class i which are not claimed by budworm induced mortality. We then have the tree update equations (applied in August at the budworm egg stage):

$$\begin{aligned} T_1(t+1) &= C + \bar{H}, \\ T_i(t+1) &= U_{i-1}, \quad i = 2,, \ldots, 74, \\ T_{75}(t+1) &= (1 - \Psi_3)(U_{74} + U_{75}). \end{aligned} \tag{2.8}$$

It remains to define the branch surface areas b and c in equation (2.7). These are given by

$$b = \sum_{i=22}^{75} T_i(t+1)\sigma_i(1 - \mu_i V), \tag{2.9}$$

where σ_i is the branch surface area of surviving susceptible trees in age class I, and $V = \min(\Psi_0 T, \Psi_1)$, where Ψ_0 and Ψ_1 are constants, and is a measure of the reduction of branch surface area due to tree stress. The branch surface area of newly susceptible trees, c, is given by $c = \sigma_{21}\bar{C}$, where $\bar{C}$ is taken as an average fraction of newly susceptible land, $\bar{C} = \frac{1}{3}(T_{20} + T_{21} + T_{22})(t+1)$.

2.5. *Dimensionless model*

Below we write the complete site model (ignoring dispersal) for the variables l, f, g, T_i, together with the subsidiary functional relationships defined above. The model is made dimensionless in the following way: the primary variables are scaled with

$$f \sim g_0, \quad g \sim g_0, \quad l \sim \frac{g_0}{c_0 \Delta t}, \tag{2.10}$$

where the choice of larval scale is based on the range over which the foliage consumption rates vary. The subsidiary variables are scaled as

$$q \sim c_0, \quad r \sim c_0, \quad u \sim g_0, \quad v \sim g_0, \quad w \sim g_0, \quad x \sim g_0,$$

$$y \sim g_0, \quad z \sim g_0, \quad k \sim \frac{g_0}{c_0 \Delta t}, \quad a \sim \frac{g_0}{c_0 \Delta t}, \quad \bar{v} \sim v_1, \quad \sigma_i \sim \sigma_{75}, \tag{2.11}$$

and the values of the constants are given in Table 1.

The dimensionless Jones site model without dispersal can then be written, where the same symbols as in (2.11) are now used to denote the corresponding variables, as

$$f(t+1) = \frac{\frac{1}{3}\lambda_1 \sum_{i=20}^{22} T_i(t+1) + \lambda_2 z \sum_{i=20}^{75} T_i(t+1)\sigma_i(1-\mu_i V)}{\frac{1}{3}\lambda_3 \sum_{i=20}^{22} T_i(t+1) + \sum_{i=22}^{75} T_i(t+1)\sigma_i(1-\mu_i V)},$$

$$g(t+1) = \frac{\frac{1}{3}\lambda_3 \sum_{i=20}^{22} T_i(t+1) + (W_1 x + W_2 y)\sum_{i=22}^{75} T_i(t+1)\sigma_i(1-\mu_i V)}{\frac{1}{3}\lambda_3 \sum_{i=20}^{22} T_i(t+1) + \sum_{i=22}^{75} T_i(t+1)\sigma_i(1-\mu_i V)},$$

$$l(t+1) = \lambda_4 \lambda_6 S w(\Theta_1 - \lambda_5 w) R \bar{v} a, \tag{2.12}$$

with

$$T_1(t+1) = T \sum_{i=22}^{75} T_i \mu_i + \Psi_3 [T_{74}(1-\mu_{74}T) + T_{75}(1-\mu_{75}T)],$$

$$T_i(t+1) = (1 - T\mu_{i-1}) T_{i-1}, \quad i = 2, \ldots, 74,$$

$$T_{75}(t+1) = (1-\Psi_3)[T_{74}(1-\mu_{74}T) + T_{75}(1-\mu_{75}T)],$$

Table 1. Parameter values (Jones 1979, except[a] Morris 1963).

Parameter	Value	Parameter	Value
Small larvae		Large larval feeding	
Θ_0	0.352	c_0	0.0074 fu ind^{-1} year^{-1}
Θ_1	2.0	Foliage update	
b_0	24000 tsf acre^{-1}	f_0	1.0 fu tsf^{-1}
Eggs		g_0	2.8 fu tsf^{-1}
E	0.81	h_0	3.8 fu tsf^{-1}
A	1.0	Spring foliage production	
Λ_3	0.289	Ω_0	0.04 tsf fu^{-1}
Λ_4	0.237	Ω_1	3.17
Fecundity		Ω_2	2.51
Σ_0	34.1	Foliage after mortality	
Σ_1	24.9	Γ_0	0.5
Σ_2	3.4	Budworm induced mortality	
Σ_3	165.64	Ψ_0	2.0
Σ_4	328.52	Ψ_1	0.8
v_0	80[a]	Ψ_2	0.75
v_1	200[a]	Removal of dead trees	
Large larvae		Ψ_3	0.0237
Φ_0	0.425	μ_i	$O(1)$
Φ_1	0.4	σ_i	$O(10^4)$ tsf acre^{-1}
Φ_2	0.003 tsf ind^{-1}	σ_{21}	17825 tsf acre^{-1}
Φ_3	2.0	σ_{75}	29500 tsf acre^{-1}
W	0.76, 1.0, 1.29		
Pupae			
Υ_0	0.473		
Υ_1	0.828		

$$q = \frac{f}{l}\left[1 - \exp\left(-\frac{l}{f}\right)\right],$$

$$r = \frac{g}{l}\left[1 - \exp\left(-(1-q)\frac{l}{g}\right)\right],$$

$$u = f\exp\left(-\frac{l}{f}\right),$$

$$v = g\exp\left(-(1-q)\frac{l}{g}\right),$$

$$w = u + v,$$

$$
\begin{aligned}
T &= \psi_2[1-v]_+^2,\\
V &= \min(\psi_0 T, \psi_1),\\
x &= \frac{u\sum_{i=22}^{75} T_i}{\sum_{i=22}^{75} T_i - \lambda_9 T\sum_{i=22}^{75} T_i\mu_i},\\
y &= \frac{v\sum_{i=22}^{75} T_i}{\sum_{i=22}^{75} T_i - \lambda_9 T\sum_{i=22}^{75} T_i\mu_i},\\
z &= \frac{w\sum_{i=22}^{75} T_i}{\sum_{i=22}^{75} T_i - \lambda_9 T\sum_{i=22}^{75} T_i\mu_i},\\
W_1 &= 1-\lambda_{10}x,\\
W_2 &= (\Omega_1-\lambda_{11}z)\lambda_5 z,\\
S &= \lambda_{12}wz(\Theta_1-\lambda_5 w)(\Theta_1-\lambda_5 z)\sum_{i=22}^{75} T_i(t+1)\sigma_i(1-\mu_i V),\\
k &= \lambda_{13}l(q+r)[1-\Phi_1\exp(-\lambda_{14}l)],\\
Q &= \sum_{j=1}^{3}\frac{A_j}{\exp\left(-\alpha_j\dfrac{k}{f+g}\right)+\beta_j\dfrac{k}{f+g}},\\
R &= \lambda_{15}+\lambda_{16}(q+r)[1-\Phi_1\exp(-\lambda_{14}l)]\\
&\quad\times\left(1+\frac{\lambda_{17}Q}{\sum_{i=22}^{75} T_i(t+1)\sigma_i(1-\mu_i V)}\right)^{-A_0},\\
\bar{v} &= \max\{\lambda_{18}(\Sigma_0 q+\Sigma_1 r-\Sigma_2)^{1/3}-\lambda_{19},\lambda_{20}\},\\
a &= \lambda_{13}l(q+r)[1-\Phi_1 e^{-\lambda_{14}l}]\left(1+\frac{\lambda_{17}Q}{\sum_{i=22}^{75} T_i(t+1)\sigma_i(1-\mu_i V)}\right)^{-A_0}\\
&\quad\times\left[\Upsilon_0+\lambda_{21}(q+r)[1-\Phi_1 e^{-\lambda_{14}l}]\left(1+\frac{\lambda_{17}Q}{\sum_{i=22}^{75} T_i(t+1)\sigma_i(1-\mu_i V)}\right)^{-A_0}\right].
\end{aligned}
\tag{2.13}
$$

The definitions of the dimensionless parameters are given in Table 2, and typical values of the parameters are given there also.

3. Reducing the model

3.1. Predation

As we have seen, one of the important mechanisms controlling budworm populations at low levels is predation by birds. Jones (1979)

Table 2. Nondimensional parameter values. The omitted values depend on unavailable data.

Parameter	Definition[a]	Value
λ_1	$f_0\sigma_{21}/g_0\sigma_{75}$	0.216
λ_2	f_0/h_0	0.263
λ_3	σ_{21}/σ_{75}	0.604
λ_4	Eg_0/h_0	0.597
λ_5	g_0/h_0	0.737
λ_6	Av_1	200
λ_9	$1-\Gamma_0$	0.5
λ_{10}	$\Omega_0 g_0$	0.112
λ_{11}	$\Omega_2 g_0/h_0$	1.849
λ_{12}	$\Theta_0\sigma_{75}g_0^2/b_0h_0^2$	0.235
λ_{13}	$\Phi_0 W$	0.323 to 0.548[b]
λ_{14}	$\Phi_2 g_0/c_0\Delta t$	1.135
λ_{15}	$\Lambda_3+\Lambda_4\Upsilon_0$	0.401
λ_{16}	$\Lambda_4\Upsilon_1\Phi_0 W$	0.063 to 0.108[b]
λ_{17}	$b_0/\Phi_3 A_0\sigma_{75}$	—
λ_{18}	Σ_3/v_1	0.828
λ_{19}	Σ_4/v_1	1.643
λ_{20}	v_0/v_1	0.4
λ_{21}	$\Upsilon_1\Phi_0 W$	0.267 to 0.454[b]
λ_{22}		0.00173
λ_{23}		0.00185
α_j	$C_j h_0/c_0\Delta t$	–
β_j	$B_j h_0/c_0\Delta t$	–

[a] In terms of dimensional quantities.
[b] Depending on the value of W.

gives no numerical values for the constants (A_j, B_j, C_j and A_0) that determine $\bar{P}$, the survival rate from predation. However, Jones's Figs. 12 and 14 give the survival probabilities before and after predation, so their ratio gives us some data for $\bar{P}$. The results lie on a smooth curve for larval densities above about 15 larvae tsf^{-1}. However, it is clear from Jones's Fig. 14 that continuing that curve downwards below 15 larvae tsf^{-1} seriously underestimates Jones's value of $\bar{P}$. There is, however, not enough data to carry out curve-fitting in that region. If we just use data for densities above 15 larvae tsf^{-1} then $\bar{P}$ is accurately represented by

$$\bar{P}=\frac{\lambda_{22}+k}{\lambda_{23}+k} \tag{3.1}$$

for constants $\lambda_{23}>\lambda_{22}>0$, and we find $\lambda_{22}=0.00173$, $\lambda_{23}=0.00904$. However, this would make $\bar{P}$ too small for small k, so we modify it by

reducing λ_{23} to 0.00185. This increases the survival probability at low k, while still providing a function that is very close to 1 for larger k. In the absence of further information we therefore proceed with $\bar{P}$ replaced by (3.1) in place of equations (2.3)–(2.4). If an alternative model of predation were proposed it could of course replace this.

3.2. *Simulation*

With these two simplifications, the site model is autonomous except for the weather factor W. We present the results of two simulations in Figs. 1 and 2. In the first of these, we take $W = 1$ (the long term average), the initial foliage levels and tree age structure to be those of a healthy forest, and the initial larval density to be $l = 0.1$. In the second case we have taken the sequence of weather factors W to be a pseudo-random sequence, with different years independent and with $W = 0.76, 1, 1.29$ having probabilities $\frac{1}{4}, \frac{1}{2}, \frac{1}{4}$. The variables plotted in the figures are f, g, l, and then three variables characterizing the tree age structure:

$$\phi(t) = T_{21}(t) \tag{3.2}$$

$$\chi(t) = \sum_{22}^{75} T_i(t) \tag{3.3}$$

$$\psi(t) = T_{74}(t) + T_{75}(t). \tag{3.4}$$

The characteristic pattern of outbreak followed by recovery is clear in each case, with Fig. 1 settling down to a period of about 50 years between consecutive outbreaks, and Fig. 2 showing similar outbreaks, irregularly spaced, with 8 outbreaks in 250 years.

3.3. *Simplification of the tree age structure*

In order to simplify the model prior to analysis, we make some approximations in the modelling of tree age structure, with the aim of representing it entirely by the variables ϕ, χ, ψ introduced above in (3.2)–(3.4). This involves making the following assumptions:

(i) the fraction of host trees becoming susceptible in a year is taken to be simply $\phi(t) = T_{21}(t)$, rather than Jones's $\bar{C}$ which averages T_{20}, T_{21} and T_{22}.

(ii) We replace all the μ_i ($22 \leqq i \leqq 75$) by their average $\mu = 0.63$, and similarly replace all the σ_i by their average $\sigma = 0.837$. This allows us to replace terms such as $\sum_{22}^{75} \mu_i T_i$ by $\mu\chi$.

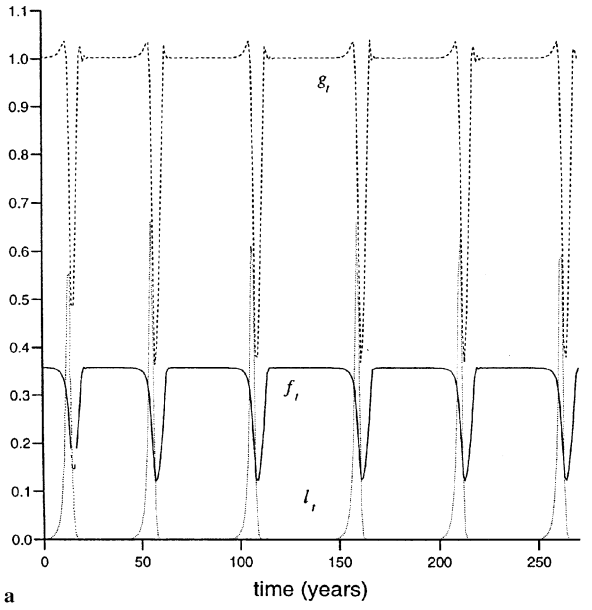

a

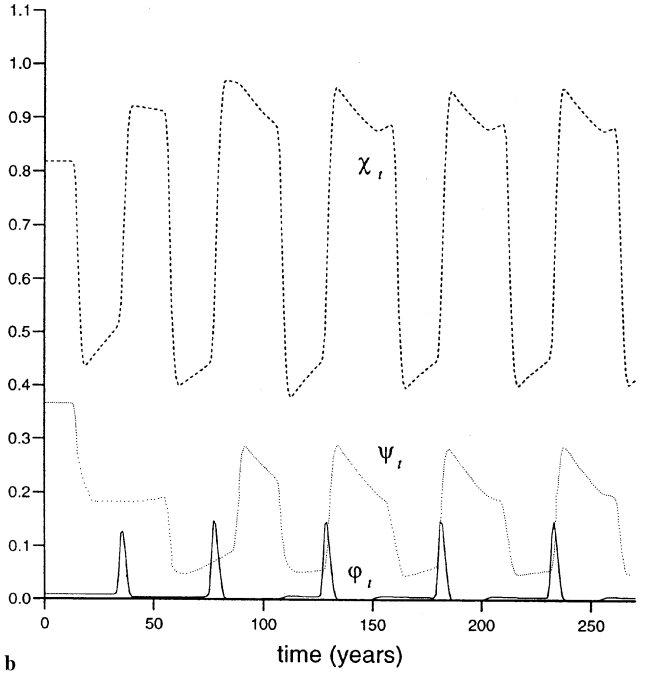

b

Fig. 1. A simulation of the full budworm site model, showing periodic outbreaks every 50 or so years. **a** The variables l (larval density), f (new foliage) and g (old foliage); **b** variation of tree age structure, represented by the variables ϕ (young trees), χ (mature trees), and ψ (old trees). The irregularity in the age structure in the first 100 years is due to the transient relaxation towards the periodic solution.

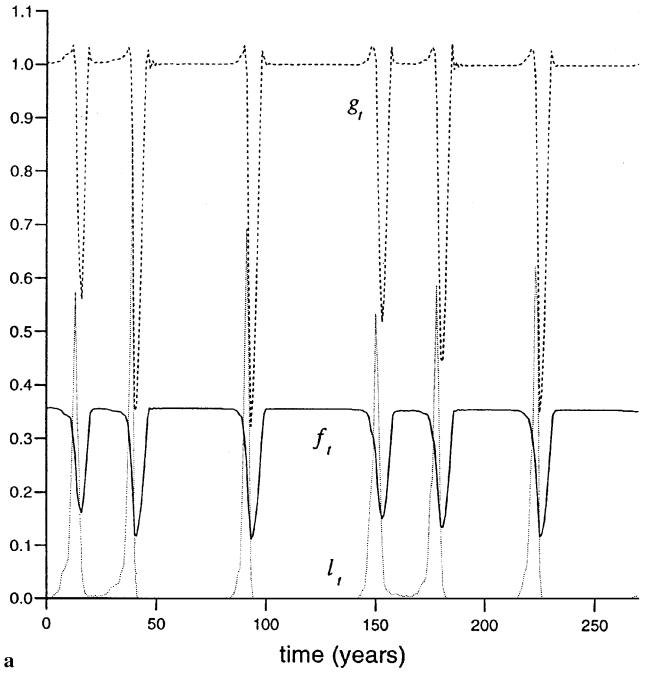

a

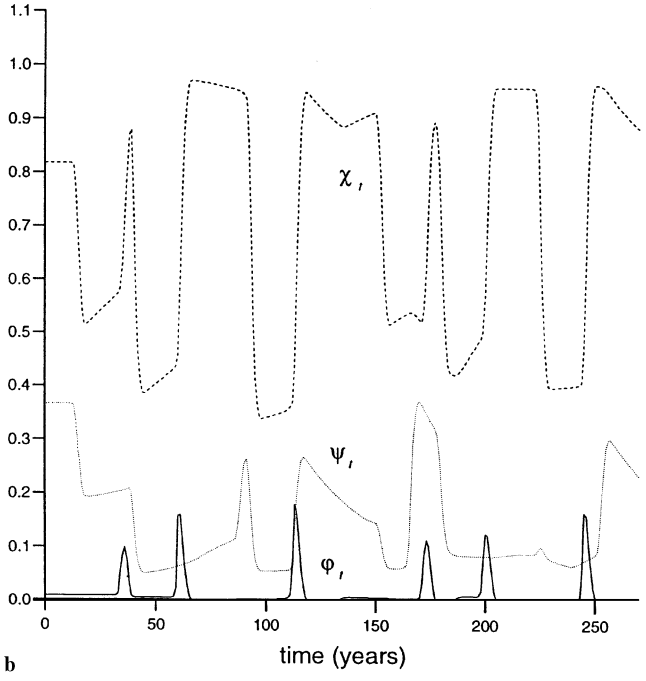

b

Fig. 2. Simulation of the full budworm site model, but allowing for a variable weather factor. **a** Larval and foliage densities; **b** tree age structure. The regular periodicity of the outbreaks is significantly affected.

(iii) We assume that the measure of trees becoming subject to natural mortality, $T_{73}(t)$, can be approximated by $\psi_4(\chi(t) - \psi(t))$, where we take $\psi_4 = 1/52$, as if trees were equally distributed between age classes 22, . . . , 73.

The tree age class equations then become

$$\phi(t+1) = \mu T(t-20)\chi(t-20) + \psi_3[1 - \mu T(t-20)]\psi(t-20),$$

$$\chi(t+1) = (1-\mu T)\chi - \psi_3(1-\mu T)\psi + \phi,$$

$$\psi(t+1) = (1-\psi_3)(1-\mu T)\psi + \psi_4(1-\mu T)(\chi - \psi). \tag{3.5}$$

3.4. Simplification of the proportion of females in the adult larval population

The value of R, the proportion of females in the adult larvae, can only vary betwen 0.401 and 0.509, and so our final simplification is to model R as constant, and in fact we choose the mean between these extremes, so the definition of R in (2.13) is replaced by

$$R = R_0 = \tfrac{1}{2}(R_{\min} + R_{\max}) = 0.455. \tag{3.6}$$

3.5. Simulation of the reduced model

The model can now be simulated with the simplifications of Sect. 3.4 and 3.5 applied, and with the same initial conditions as for Figs. 1 and 2. The results are shown in Figs. 3 and 4, again plotting f, g, l, ϕ, χ and ψ. The results are in good agreement, and we therefore proceed in our analysis by looking at the simplified model.

4. An analysis of the reduced model

The simplified model is still of daunting complexity, and in this section we aim to provide some insight into its behaviour. Our starting point is the observation that the larval scale $g_0/c_0\Delta t \approx 378\,\text{ind}\,\text{tsf}^{-1}$ is much higher than observed values between outbreaks, but also less than the maximum values obtained during an outbreak. Moreover, the numerical simulations of the preceding section indicate that between outbreaks, the dimensionless larvae variable l becomes very low. This motivates our initial investigation of (3.1) and (3.2), based on the limit where $l \ll 1$.

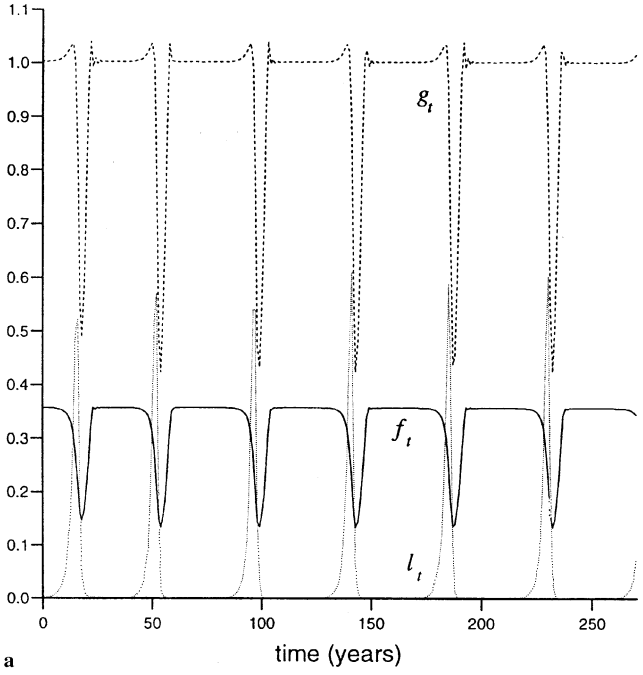

a

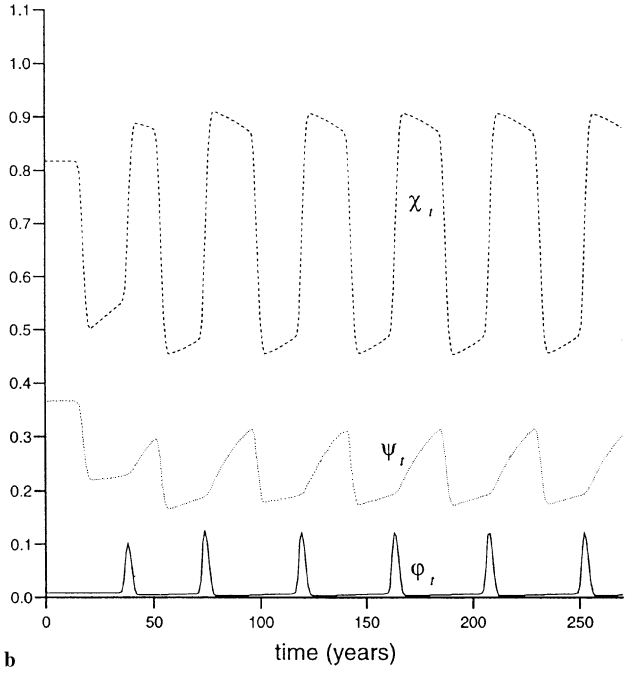

b

Fig. 3. Simulation of the site model as in Fig. 1, but with R constant, and with the reduced tree age structure equations (3.5). **a** Larval and foliage densities; **b** tree age structure.

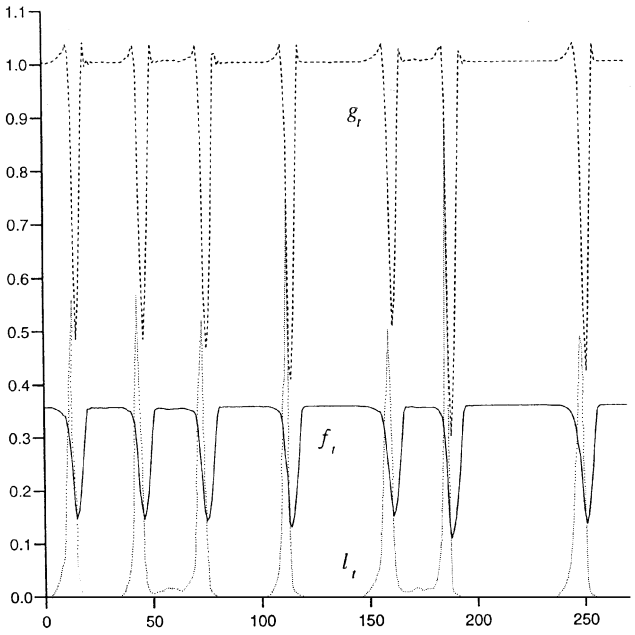

a

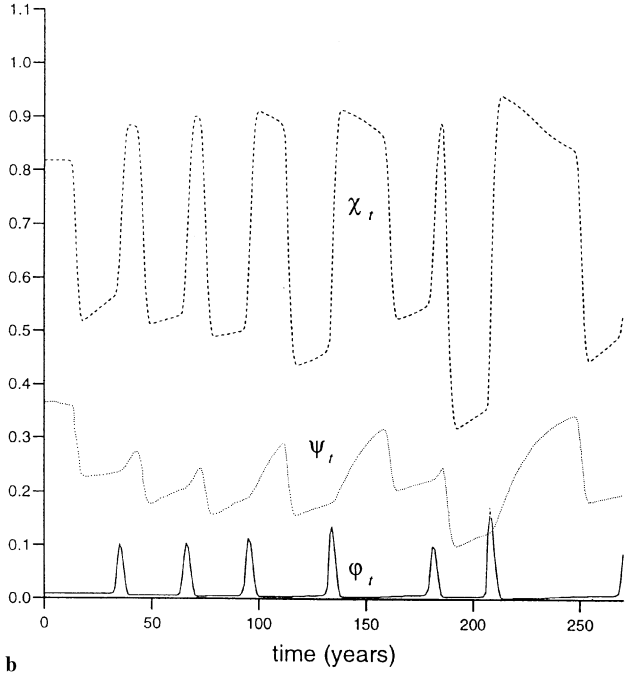

b

Fig. 4. Simulation of the reduced 6 variable site model as for Fig. 3, but with variable weather, as in Fig. 2. **a** Larval and foliage densities; **b** tree age structure.

Expanding the exponential terms in (3.2) for $l \ll 1$, we find that

$$q \approx 1, \qquad r \approx 0,$$

$$u \approx f, \qquad v \approx g, \qquad w \approx f + g,$$

$$T \approx \Psi_2[1-g]_+^2, \qquad V = \min(\Psi_0 T, \Psi_1),$$

$$x \approx \frac{f}{1-\lambda_9\mu T}, \qquad y \approx \frac{g}{1-\lambda_9\mu T}, \qquad z \approx \frac{f+g}{1-\lambda_9\mu T},$$

$$W_1 \approx 1 - \lambda_{10}\frac{f}{1-\lambda_9\mu T}, \quad W_2 \approx \lambda_5\frac{f+g}{1-\lambda_9\mu T}\left(\Omega_1 - \lambda_{11}\frac{f+g}{1-\lambda_9\mu T}\right),$$

$$S \approx \lambda_{12} wz(\Theta_1 - \lambda_5 w)(\Theta_1 - \lambda_5 z)\sigma(1-\mu V)\chi(t+1),$$

$$k \approx \lambda_{13}(1-\Phi_1)\,l, \qquad \bar{v} \approx \lambda_{18}(\Sigma_0 - \Sigma_2)^{1/3} - \lambda_{19},$$

$$a \approx \frac{\lambda_{22}\lambda_{13}(1-\Phi_1)l}{\lambda_{23}}\left[\Upsilon_0 + \frac{\lambda_{22}\lambda_{21}(1-\Phi_1)l}{\lambda_{23}}\right], \tag{4.1}$$

and we use these approximations below.

Foliage submodel. If l is low for a long time, then we expect the forest to become healthy, and in particular we can expect $\phi \ll \chi$. So long as this is the case, the foliage update equations can be written in the form (with $f(t) = f_t$, etc.)

$$f_{t+1} = \lambda_2 \frac{f_t + g_t}{1 - \lambda_{25}[1-g_t]_+^2},$$

$$g_{t+1} = \frac{f_t}{1-\lambda_{25}[1-g_t]_+^2}\left(1 - \lambda_{10}\frac{f_t}{1-\lambda_{25}[1-g_t]_+^2}\right)$$
$$+ \lambda_5 \frac{g_t(f_t+g_t)}{[1-\lambda_{25}[1-g_t]_+^2]^2}\left(\Omega_1 - \lambda_{11}\frac{f_t+g_t}{1-\lambda_{25}[1-g_t]_+^2}\right), \tag{4.2}$$

where $\lambda_{25} = \lambda_9\mu\Psi_2 \sim 0.24$. We see that f and g uncouple from the rest of the system, and we would hope that they would reach a stable steady state, corresponding to a healthy forest. Indeed, the healthy state $(f_0/g_0, 1)$ is a steady state of (4.2), and by linearising about this state, we find that with the parameter values quoted it is stable. There is in fact another equilibrium at (0.038, 0.078), but it is unstable. Figure 5 shows a numerical simulation of (4.2) showing the nonlinear approach to the healthy equilibrium.

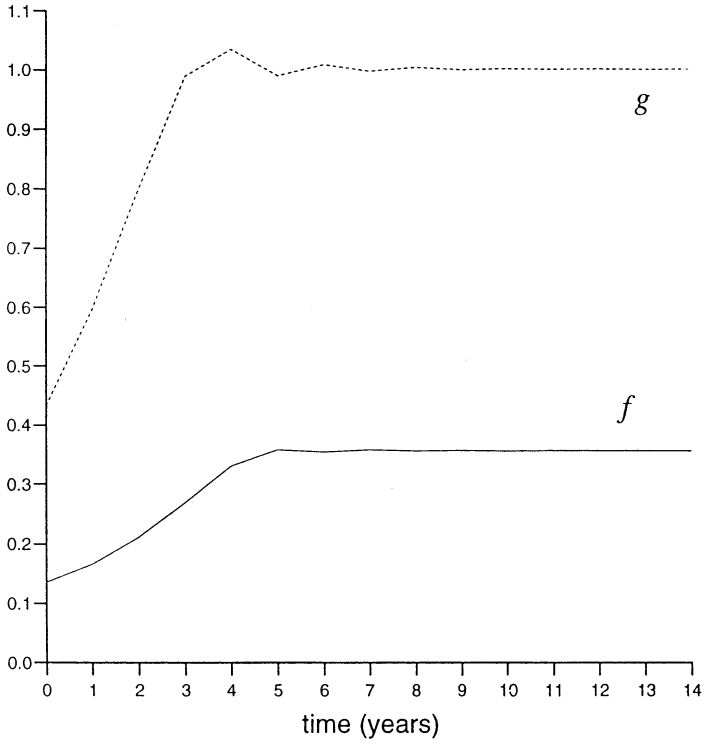

Fig. 5. Relaxation of foliage towards equilibrium when larval density is low.

Tree update model. When $l \ll 1$, we have $v \approx g$, and in healthy equilibrium, $g = 1$, so that $T = 0$, and the tree age structure is governed by the simplified system

$$\begin{aligned} \phi_{t+1} &= \Psi_3 \psi_{t-20}, \\ \chi_{t+1} &= \chi_t - \Psi_3 \psi_t + \phi_t, \\ \psi_{t+1} &= (1 - \Psi_3)\psi_t + \Psi_4(\chi_t - \psi_t). \end{aligned} \tag{4.3}$$

This is a linear homogeneous system of equations, to which we adjoin an equation describing conservation of host tree area, leading to

$$\chi_t + \sum_{j=0}^{20} \phi_{t+j} = 1 \tag{4.4}$$

for all t (and which is consistent with (4.3)). The system (4.3) has a unique steady state given by

$$\begin{aligned} (\phi^*, \chi^*, \psi^*) &= \frac{\Psi_5}{\Psi_3\Psi_4 + \Psi_5(\Psi_3 + \Psi_4)}(\Psi_3\Psi_4, \Psi_3 + \Psi_4, \Psi_4) \\ &\approx (0.009, 0.818, 0.366), \end{aligned} \tag{4.5}$$

where $\Psi_5 = 1/21$ and we see that in the steady state $\phi \ll \chi$, as assumed. The stability is ascertained by firstly writing (4.3) as the 23rd order system

$$\begin{pmatrix} \phi_{t+1} \\ \chi_{t+1} \\ \psi_{t+1} \\ \psi_t \\ \vdots \\ \psi_{t-19} \end{pmatrix} = \begin{pmatrix} 0 & 0 & 0 & 0 & & \Psi_3 \\ 1 & 1 & -\Psi_3 & 0 & \cdots & 0 \\ 0 & \Psi_4 & 1-\Psi_3-\Psi_4 & 0 & & 0 \\ 0 & 0 & 1 & 0 & & 0 \\ & \vdots & & \ddots & & \vdots \\ 0 & 0 & 0 & \cdots & 1 & 0 \end{pmatrix} \begin{pmatrix} \phi_t \\ \chi_t \\ \psi_t \\ \psi_{t-1} \\ \vdots \\ \psi_{t-20} \end{pmatrix}. \tag{4.6}$$

the matrix of which has one eigenvalue of 1 (due to (4.4)), and the rest less than 1 in magnitude. The steady state (4.5) is therefore stable, as we should expect. Figure 6 shows a numerical simulation of the approach to steady state of the tree age structure.

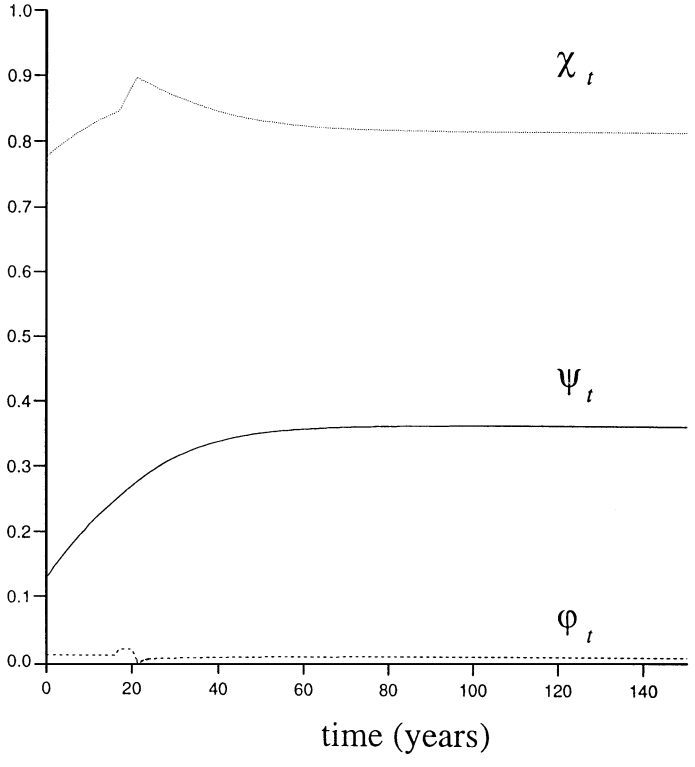

Fig. 6. Relaxation of tree age structure towards equilibrium when larval density is low and foliage is at equilibrium.

Larval regeneration. Taking the approximations in (4.1), and assuming $W = 1$ (average weather conditions), the large larval update equation becomes

$$l_{t+1} = \rho_0 l_t, \tag{4.7}$$

where the growth rate ρ_0 is given by

$$\rho_0 = \frac{\lambda_{26}\lambda_{22}}{\lambda_{23}}\left[\Upsilon_0 + \frac{\lambda_{21}(1-\Phi_1)\lambda_{22}}{\lambda_{23}}\right], \tag{4.8}$$

and

$$\lambda_{26} = \lambda_{12}\lambda_{13}\lambda_{24}\bar{v}\sigma\chi^*(1-\Phi_1)\left(\frac{f_0}{g_0}+1\right)^3\left[\Theta_1 - \lambda_5\left(\frac{f_0}{g_0}+1\right)\right]^3$$

$$= 5.29, \tag{4.9}$$

λ_{24} being given by $\lambda_4\lambda_6 R_0 \approx 54.3$.

The parameter ρ_0 identifies the first critical bifurcation parameter of our analysis. If $\rho_0 < 1$, then we expect small larval populations to die away, whereas if $\rho_0 > 1$, the larval population will grow exponentially. For the parameter values we adopt here, we find $\rho_0 \approx 3.3$, and growth is predicted.

Larval collapse. If oscillations occur, then we should not only expect growth at low l, but collapse at high l. Approximation of the system when l is large in (3.2) suggests $v \ll 1$, hence $w, S \ll 1$, and thus (from (3.1)) $l_{t+1} \ll 1$, but this gives no details of the collapse or the subsequent regeneration, although it is suggestive. On the other hand, it is quite possible that the growth of l from small values could lead to an endemic equilibrium, with $l \sim 1$.

4.1. The three-variable outbreak model

In order to try and get some insight into the nature of the outbreak and subsequent collapse, we are led to consider further simplification of the model with the aim of removing inessential detail.

Tree age structure. Previously, we assumed $\phi \ll \chi$, and Fig. 6 suggests this is in fact always reasonable. Also the mortality/generation and age parameters Ψ_3 and Ψ_4 are small, and if we neglect these then the tree age equations in (3.1) condense to

$$\begin{aligned} \chi_{t+1} &= (1-\mu T)\chi_t, \\ \psi_{t+1} &= (1-\mu T)\psi_t, \end{aligned} \tag{4.10}$$

of which the ψ equation uncouples from consideration of χ. Note that the loss of the term in Ψ_3 precludes regeneration, which would be necessary to describe any subsequent recovery of the forest.

Foliage update. In healthy forest, $f \to f_0/g_0 \approx 0.4$ while $g \to 1$. More generally, $f < g$, and Figs. 2 and 3 suggest further that essentially the behaviour of f follows that of g, in the sense that f/g is roughly constant. This suggests that the distinction between new and old foliage is a cosmetic detail, and we choose to simplify the model by putting f/g to zero (formally, based on the limit $f_0/g_0 \ll 1$). With $f \approx 0$, we then have $q, u, x \approx 0$, and

$$\begin{aligned} w, y, z &\approx v = g \exp(-l/g), \\ W_1 &\approx 1, W_2 \approx \lambda_5 v(\Omega_1 - \lambda_{11} v), \end{aligned} \tag{4.11}$$

so that, with $\phi \ll \chi$, the foliage dynamics may be represented as

$$g_{t+1} = W_1 x + W_2 y \approx \lambda_5 v^2(\Omega_1 - \lambda_{11} v) = H(v). \tag{4.12}$$

Larval growth. During the outbreak, predation and parasitism are ineffective, and we take the respective survival rates as 1. In addition, we suppose $\bar{v} \approx 0.68$, $V \approx 0.4$ to be constant. Adopting the foliage assumptions, the larval growth equation can be written as

$$l_{t+1} = F(v) G(l_t/g_t) \chi_{t+1} l_t, \tag{4.13}$$

where

$$\begin{aligned} F(v) &= \lambda_{12}\lambda_{13}\lambda_{24}\sigma\bar{v}(1 - \mu V) v^3 (\Theta_1 - \lambda_5 v)^3, \\ G(x) &= \frac{1}{x}(1 - \mathrm{e}^{-x}) \left[\Upsilon_0 + \frac{\lambda_{21}}{x}(1 - \mathrm{e}^{-x}) \right]. \end{aligned} \tag{4.14}$$

In both (4.12) and (4.13), v (defined in (4.11)) is v_t, i.e., evaluated at time t.

The form of these functions, F, G and H, is of course determined by the precise ecological assumptions involved. We adopt the point of view that it is the qualitative form of these functions which is most important. In particular, $G(\xi)$ is a monotone decreasing function of ξ, and we choose now to take $G(\xi) = e^{-\xi}$ (the more general $G = c_1 e^{-c_2 \xi}$ allows a similar analysis), which is convenient and no less appropriate. Since $\exp(-l/g) = v/g$, the choice of G allows $G(l/g) = v/g$, thus (4.13), together with (4.12) and $(4.10)_1$, become

$$\begin{aligned} l_{t+1} &= v_t F(v_t) \chi_{t+1} l_t/g_t, \\ g_{t+1} &= H(v_t), \\ \chi_{t+1} &= (1 - \mu T)\chi_t, \end{aligned} \tag{4.15}$$

with

$$v_t = g_t \exp(-l_t/g_t),$$
$$T = \Psi_2[1 - v_t]_+^2. \tag{4.16}$$

4.2. Larvae-foliage outbreak

In order to discuss the three variable model derived above, we begin by considering $\chi_t = \chi^*$ as constant. Insofar as it is only coupled as a reduction factor in $(4.15)_1$, its rôle does not seem essential to control of the outbreak. Formally, this can be justified if μ is small. From (4.15), we then have, if we define $L_t = l_t/g_t$ (essentially larvae per foliage unit),

$$L_{t+1} = \chi^* K(v_t) L_t, \tag{4.17}$$

where

$$K(v) = \frac{vF(v)}{H(v)}, \tag{4.18}$$

and

$$v_{t+1} = H(v_t) e^{-L_{t+1}}. \tag{4.19}$$

Solving (4.17) and (4.19) for L and v gives g and l via $g = ve^L$, $l = Lve^L$, both of which are monotonic increasing functions of both v and L.

From its definition in (4.12), we see that H is bell-shaped in the physically meaningful range $0 < v < \Omega_1/\lambda_{11} \approx 1.7$, with the Allee effect that $H \sim v^2$ as $v \to 0$. It is represented in Fig. 7. To represent the behaviour relevant in practice, we also assume that there is a certain range in which $H(v) > v$, otherwise (4.19) inevitably makes $v_t \to 0$.

F is also bell shaped in $0 < v < \Theta_1/\lambda_5 \approx 2.7$, and $F \sim v^3$ as $v \to 0$. If we adopt these values, in particular that $\Omega_1/\lambda_{11} < \Theta_1/\lambda_5$, then it seems that K will be monotone increasing, with $K \sim v^2$ as $v \to 0$, and $K \to \infty$ as $v \to \Omega_1/\lambda_{11}$, as shown in Fig. 8. We denote the unique solution of $\chi^* K(v) = 1$ by $v = v_K$, so v_K is the steady foliage level that would just sustain a steady budworm population : L will grow for $v > v_K$ and decay for $v < v_K$. The value of v_K itself is a decreasing function of χ^* : the higher the density of mature trees in a forest, the lower the value of v_K. Note that for an initial state which is healthy, then $v \approx g \approx 1$.

Slowly varying L. It is now convenient to think of L as varying slowly. Formally, this will be the case if $v \approx v_K$, and in practice we consider it a convenience rather than a necessary assumption. The point is that if we take L_{t+1} as a parameter in (4.19), the behaviour of v_t is easily ascertained. Because of the properties of H, there will be a critical value $L_H > 0$ such that if $L = L_H$ then the graphs of v and $H(v)e^{-L}$ are tangent at some value $v = v_H$ as in Fig. 7. In fact v_H is the foliage level

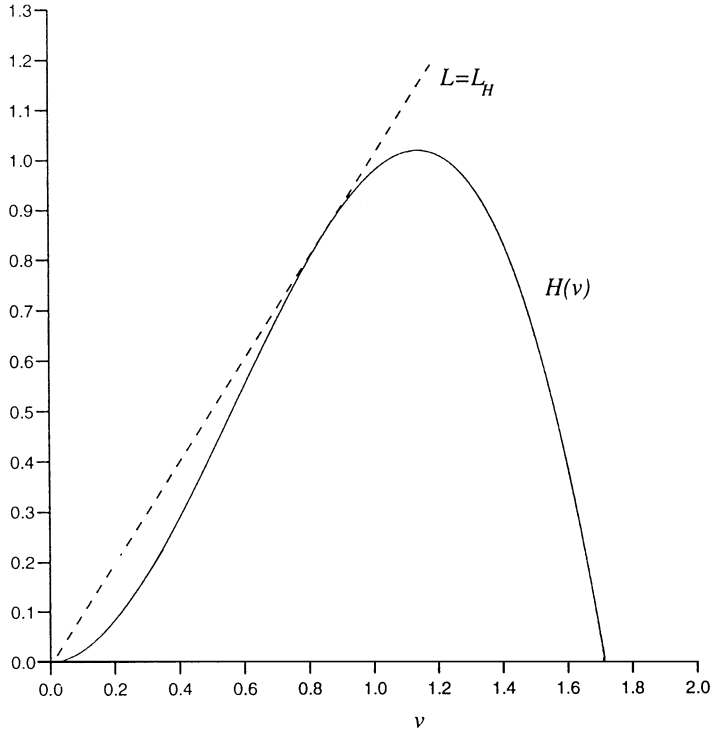

Fig. 7. $H(v)$ as a function of v, given in equation (4.12). Also plotted is the graph of ve^L at the critical value $L = L_{\mathrm{H}}$ for tangency.

for which the foliage growth factor in a healthy (budworm-free) forest, $H(v)/v$, would be maximized; and L_H is the budworm/foliage ratio that would be just enough to reduce this maximum foliage growth factor down to 1, so

$$1 < \max(H(v)/v) = H(v_{\mathrm{H}})/v_{\mathrm{H}} = H'(v_{\mathrm{H}}) = e^{L_H}. \tag{4.20}$$

We may call v_H the growth-maximizing foliage level. If $L < L_H$ then the foliage equation (4.19) will have two positive steady states. The greater of these, denoted by v_+ (a function of L), is stable and is therefore hunted by v_t. If $L > L_H$, the two positive steady states collapse in a saddle-node bifurcation and there is an irreversible decline of v towards zero. In fact, L_H is the largest steady budworm density that can be sustained.

For H given by (4.12), v_H and L_H are given by

$$v_H = \frac{\Omega_1}{2\lambda_{11}}, \qquad L_H = \ln\left[\frac{\lambda_5 \Omega_1^2}{4\lambda_{11}}\right]. \tag{4.21}$$

With the present values, $v_H \approx 0.85$, $L_H \approx 0.001$.

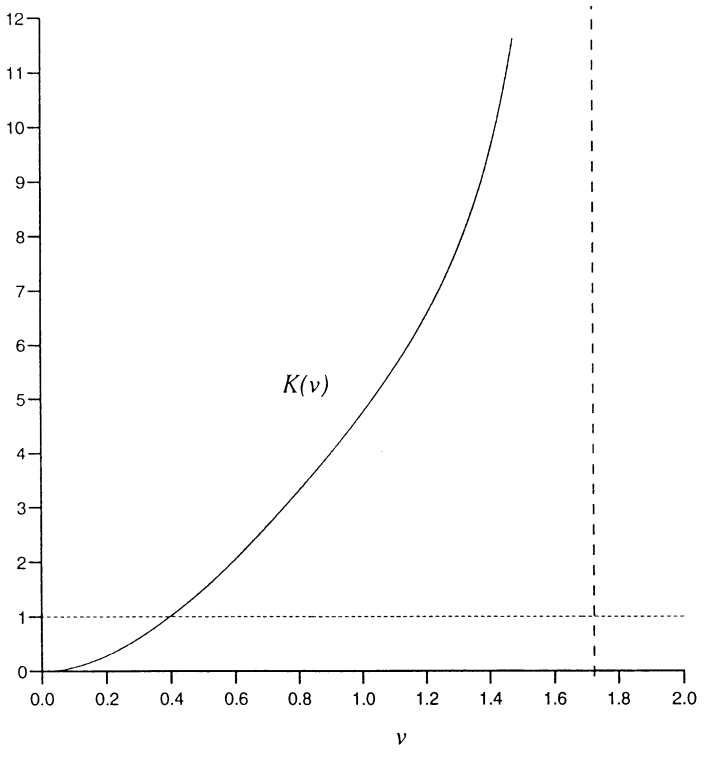

Fig. 8. $K(v)$ given by equation (4.18).

Let us now suppose that $0 < L \ll L_H$ initially; then v hunts the upper positive steady state v_+, and we denote the value of v_+ for $L = 0$ by v_+^0: this is the largest solution of $H(v) = v$, it is the steady foliage level in a healthy forest, and in the present instance it is given by

$$v_+^0 = v_H[1 + (1 - e^{-L_H})^{1/2}]. \tag{4.22}$$

We always have $v_+^0 > v_H$, but there are three possible behaviours that can arise depending on whether v_K lies above, between or below these values v_H and v_+^0.

If $v_K > v_+^0$ then $K(v) < 1$, L decays, and thus L remains less than L_H, v remains near v_+, and the larvae cannot grow. This would correspond to the case $\rho_0 < 1$ considered above.

If $v_H < v_K < v_+^0$ then initially v hunts v_+, $\chi^* K(v_+) > 1$, so that L grows. This growth will continue while $\chi^* K > 1$, i.e. while $v > v_K$, i.e. while $v_+ > v_K$. As L increases, the stable positive intersection at v_+ of $H(v) = ve^L$ is decreasing. Since $v_H < v_K$, v_+ will reach v_K and we expect a stable endemic equilibrium value $v = v_K$ to occur, with $L = \ln[H(v_K)/v_K]$.

If $v_K < v_H$ then the process is similar, except that as L increases, v_+ reaches v_H and the saddle-node transition occurs, leading to a drastic reduction in v. Of course, once $v < v_K$, L then decreases, but once v is past the transition, its decay cannot be helped. This corresponds to collapse of the outbreak, with both L and v (hence also g and l) tending to zero. Since regeneration has been specifically excluded, there is no possibility for further outbreaks.

Summary. We have introduced three important foliage levels:

v_+^0 is the steady state foliage level in a healthy forest, so it is the largest solution of $H(v) = v$.

v_H is the foliage level that maximizes the foliage growth factor $H(v)/v$.

v_K is the foliage level that will just sustain a budworm population, so $\chi^* K(v_K) = 1$.

We always have $v_H < v_+^0$, and the behaviour of the system starting from a low value of L depends on how v_K compares with v_H and v_+^0. The value of v_K itself depends on χ^*, the density of mature trees, and three cases can occur:

Case 1: If the density of mature trees is low enough, then the healthy foliage level is below that necessary to sustain a budworm population, $v_+^0 < v_K$, and the larval population then collapses with no outbreak occurring.

Case 2: If the density of mature trees is in an intermediate range, then $v_H < v_K < v_+^0$, so the healthy foliage level can sustain a budworm population, but the growth-maximizing foliage level cannot. In this case, a stable endemic equilibrium is expected.

Case 3: If the density of mature trees is large enough, then $v_H > v_K$, i.e. the growth-maximizing foliage level exceeds that necessary to sustain a budworm population. In this case the analysis predicts a budworm outbreak followed by a collapse.

Figures 9, 10 and 11 show numerical simulations of the reduced model, which illustrate (for differing parameter values) the three possibilities outlined above: larval collapse, an endemic state, or an outbreak.

4.3. Variable age structure

The question now arises, how the inclusion of a variable age structure modifies the discussion above. We can write the system (4.15) in the

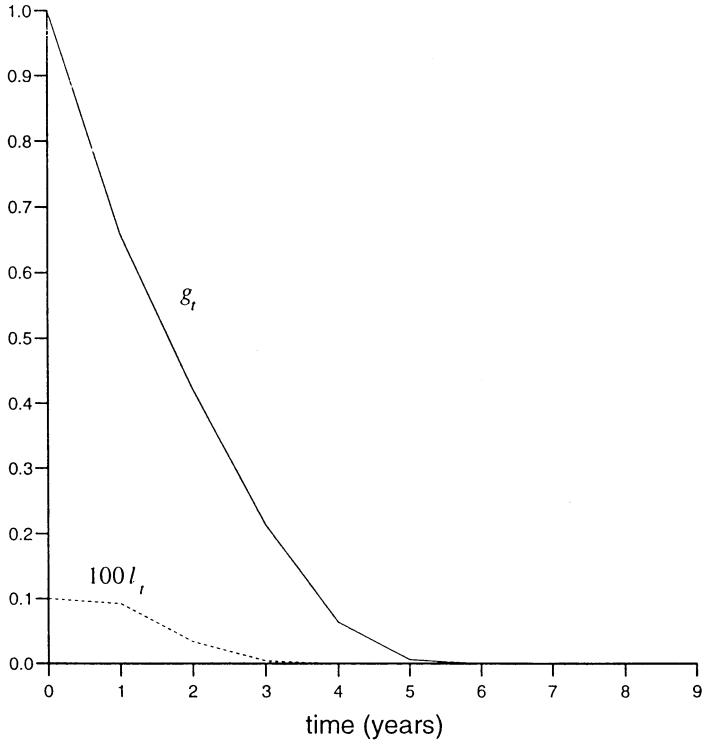

Fig. 9. The two-variable larvae/foliage reduced model; larval collapse occurs when $\lambda_{24} = 8.0$, $\lambda_5 = 0.5$.

form

$$\begin{aligned} \chi_{t+1} &= m(v_t)\chi_t, \\ H(v_t) &= v_{t+1}e^{L_{t+1}}, \\ L_{t+1} &= \chi_{t+1}K(v_t)L_t, \end{aligned} \tag{4.23}$$

adopting the previous definitions, where the survival function $m(v)$ is given by

$$m(v) = 1 - \mu\Psi_2[1 - v]_+^2, \tag{4.24}$$

and is monotone increasing from $m(0) < 1$ to $m = 1$ for $v \geqq 1$.

In particular, χ_t is non-increasing with t, and thus the function $\chi_{t+1}K(v)$ increases with v from zero to infinity as before, but decreases as t increases (if $v < 1$). Defining v_t^K as the unique value where $\chi_{t+1}K(v) = 1$, we see that v_t^K increases with t (if $v < 1$).

Compared with the system described in Sect. 4.2, the constant v_K has been replaced by v_t^K which increases as the density of mature

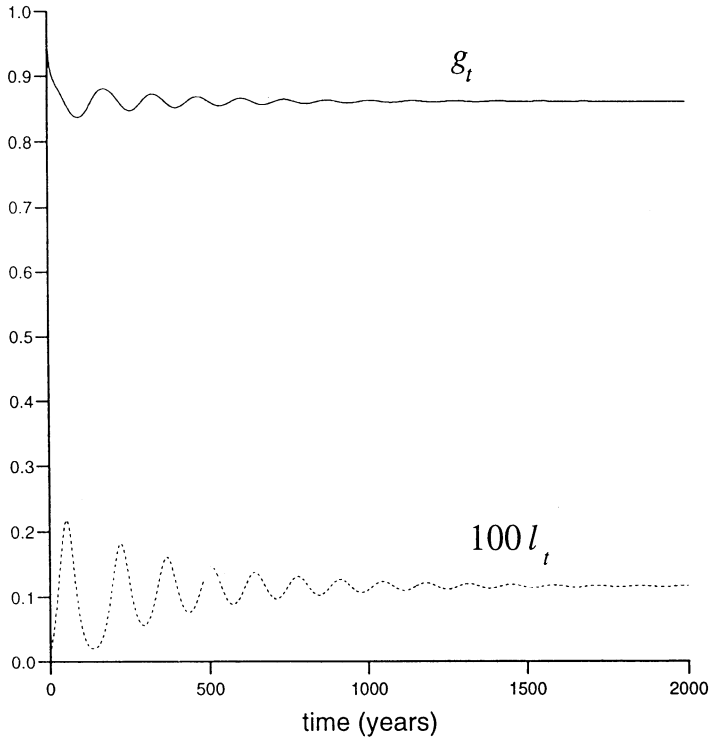

Fig. 10. Two-variable reduced model, endemic state when $\lambda_{24} = 17.9$.

trees in the area falls. The behaviour of the system can therefore be classified using the results of the previous section.

We saw in Sect. 4.2 that in order for an outbreak followed by a collapse to occur it was necessary to have $v_K < v_H$. In the case presently under consideration, it will be necessary not only that the initial value v_0^K of v_K should be less than v_H, but also that the rising value of v_t^K should not reach v_H before the outbreak occurs. Thus if v_0^K is sufficiently far below v_H then an outbreak-collapse response would be expected. As before, this requires a high enough initial density of mature trees.

If v_0^K is large enough to avoid this possibility, then v_t^K exceeds v_H at some time, and then a further division of cases occurs, depending on how the range $[v_H, v_+^0]$ lies with respect to $v = 1$, the critical foliage level needed to maintain the density of mature trees in the forest.

1. If $1 < v_H$ then both Cases 2 and 3 described in section 4.2 occur essentially unchanged : either endemic equilibrium if the initial

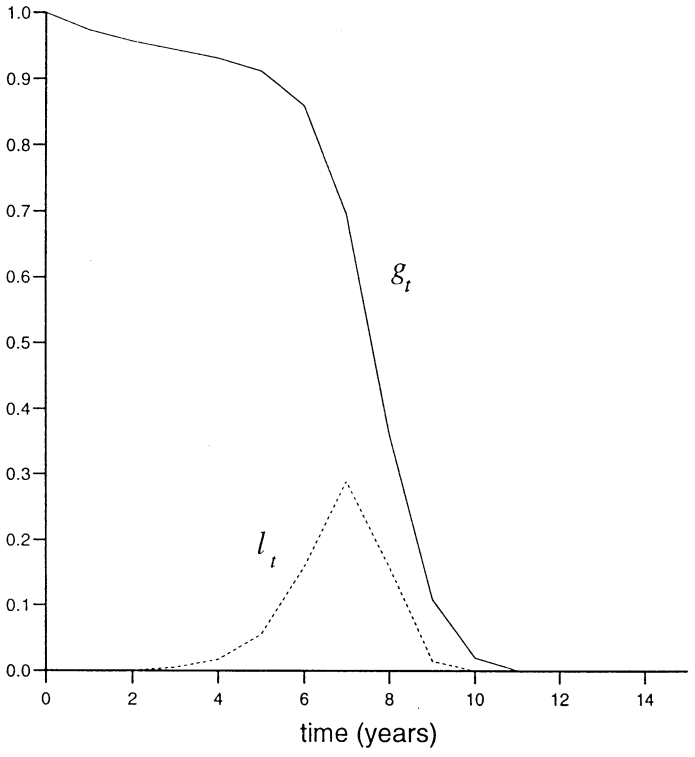

Fig. 11. Two-variable reduced model, outbreak at normal parameter values.

density of mature trees is in an intermediate range, or a budworm collapse if it is low enough.

2. If $v_H < 1 < v_+^0$ then there is a modification because the endemic equilibrium states (v, L) with $v < 1$ are not now equilibria of the χ equation. In fact, when $v < 1$, χ will decrease steadily, and so v_K will rise steadily, and the endemic equilibrium states of (4.17)–(4.19) with $v < 1$ will move along to some value of $v \geqq 1$. Thus the behaviour is similar to Cases 2 and 3 of Sect. 4.2, except that the endemic equilibria now only occupy the range $1 \leqq v \leqq v_+^0$, rather than the whole range $v_H \leqq v \leqq v_+^0$.
3. If $v_+^0 < 1$ then the whole range of endemic equilibria is lost, and the only behaviour possible apart from outbreak-collapse, is a simple collapse. However, this collapse involves the χ^* dynamics in an essential way, and so may take place over a longer timescale than the collapse that results simply from the budworm-foliage interaction in Case 3 of Sect. 4.2.

Summary. The behaviour is essentially as discussed in Sect. 4.2, but with these modifications:

1. If the growth-maximizing foliage level is not enough to sustain the density of mature trees, $v_H < 1$, then the stable endemic equilibrium conditions can only occur for $1 \leqq v \leqq v_+^0$, not for the whole range of foliage levels $v_H \leqq v \leqq v_+^0$ that occurred in Case 2 of Sect. 4.2.
2. If additionally the healthy equilibrium foliage level is not enough to sustain the density of mature trees, $v_+^0 < 1$, then no range of stable endemic state occurs at all, and the intermediate Case 2 of 4.2 is replaced by an initially slow decline in the forest, as the density of mature trees falls, followed by a more rapid decline once $\chi^* = 1/K(v_+^0)$ is reached.

5. Discussion

One shortcoming of the two-variable outbreak model (4.17) and (4.19) is the fact that an outbreak is followed by collapse, with both larval density (l) and foliage density (v and g) tending to zero. The reason for this is, of course, that we have simplified the model by ignoring the (small) regeneration terms. Thus in order to obtain cyclic oscillations, a regeneration mechanism must be included. Our initial efforts to do this, by including trees entering maturity ($\phi(t) = T_{21}(t)$) in some way, failed abysmally. In fact, age structure is only really relevant insofar as the reason for the collapse of foliage density in (4.19) is the quadratic behaviour of H as $v \to 0$. In turn, this stems from (4.12), which arises through neglecting the new foliage (f) terms in (4.2), and, more germanely, neglecting the term due to trees entering maturity in the foliage update equation $(2.12)_2$. Although the new foliage terms render the foliage model (hence, in effect, H) linear at small foliage density, they do not regenerate the forest on their own. Indeed, the Jones site model specifically caters for the fact that foliage-poor trees will fail to grow new foliage due to lack of photosynthesis. Thus merely including new foliage in (4.12) is not the remedy we seek.

We thus modify the reduced two-variable model at low foliage levels by writing (2.12) in the form (for small ϕ)

$$g_{t+1} = \frac{\lambda_3 \phi_{t+1}}{\sigma(1 - \mu V)\chi_{t+1}} + H(v_t), \tag{5.1}$$

noting that $v_t \approx g_t$ when g_t is small. A uniform approximation to the two-variable model allowing for regeneration is then (4.17) as before, together with

$$v_{t+1} = [\gamma + H(v_t)]e^{-L_{t+1}}, \tag{5.2}$$

where

$$\gamma = \frac{\lambda_3 \phi}{\sigma(1 - \mu V)\chi}. \tag{5.3}$$

We take γ as constant, although it will vary in reality. With values $\lambda_3 = 0.604$, $\sigma = 0.837$, $\mu = 0.63$, $V = 0.4$, $\phi = \phi^* = 0.009$, $\chi = \chi^* = 0.818$, the latter pair corresponding to equilibrium tree age structure at low larval levels, then $\gamma \approx 0.011$. At such a low value, the model appears not to oscillate, or at least not on a sensible time scale. Figure 12 shows a typical oscillation which occurs when $\gamma = 0.135$. Note that in both the full and reduced (6 variable) models (see Figs. 1 and 3), the value of χ during recovery is nearer $\chi = 0.4$, and if we use

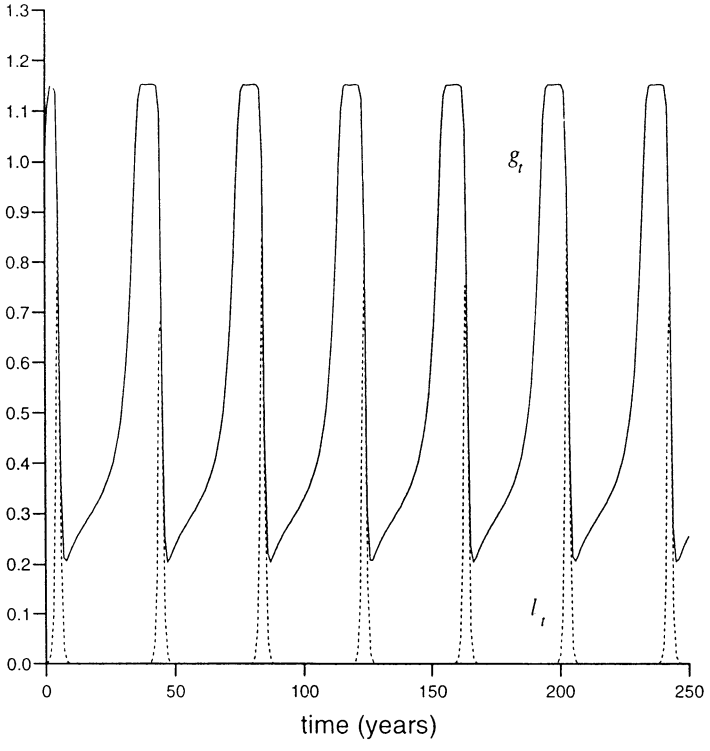

Fig. 12. Two-variable reduced model plus regeneration, equations (4.17) and (5.2); oscillations occur at a value $\gamma = 0.135$.

(4.4) to define

$$\phi = \Psi_5(1 - \chi), \tag{5.4}$$

then the resulting value of γ which we compute is in fact 0.07.

In order to accommodate a larger value of γ more realistically, we can include the equation for χ_{t+1} as in $(4.23)_1$, but we then also need to include a regeneration term for χ comparable to that for the foliage. Thus we pose a reduced three variable model of the form

$$\begin{aligned} L_{t+1} &= \chi_{t+1} K(v_t) L_t, \\ v_{t+1} &= \left[\frac{\bar{\gamma}(1 - \chi_{t+1})}{\chi_{t+1}} + H(v_t) \right] e^{-L_{t+1}}, \\ \chi_{t+1} &= m(v_t)\chi_t + \Psi_5(1 - \chi_t), \end{aligned} \tag{5.5}$$

where $\bar{\gamma}$ is defined by

$$\bar{\gamma} = \frac{\lambda_3 \Psi_5}{\sigma(1 - \mu V)} \approx 0.046. \tag{5.6}$$

Figure 13 shows oscillatory outbreaks in a solution of these equations.

We can now easily understand the cause of the oscillation (for the two variable model) in terms of Fig. 14, which indicates the shape of the curve $\gamma + H(v)$ as a function of v. As before, slow growth of L at large v causes a steepening of the line $e^L v$ in the figure, and a collapse occurs if L reaches L_H. However, for $\gamma > 0$, v now rapidly approaches a quasi-stable steady state at low v (≈ 0.2 in Fig. 14). This in turn causes rapid collapse of L. With $\gamma > 0$, there is now a further critical value $L_\gamma > L_H$ where the low v quasi-equilibrium disappears and v grows again towards the large quasi-steady state. The cycle then repeats itself.

This description of the oscillation, via the cycling round a hysteresis loop for v via slow responsive changes in L, is tantalisingly similar to the Ludwig–Jones–Holling (LJH) continuous model, but there are important differences. Most obviously, the LJH model apparently concerns hysteresis in the larval population, whereas that here is associated with foliage. In an analysis of the LJH model, Fowler (1997) shows that for the parameters which apply in the LJH model, both B (the larval population) and E (the energy reserve, or foliage variable) are fast, and each has a hysteretic dependence: B varies hysteretically with S, the branch surface area, which should be analogous to χ here; E varies hysteretically with B. This second hysteresis loop corresponds to that which we describe here.

Perhaps a clearer comparison can be made if we write the continuous equivalents of (4.15). With the definition of K in (4.18), and

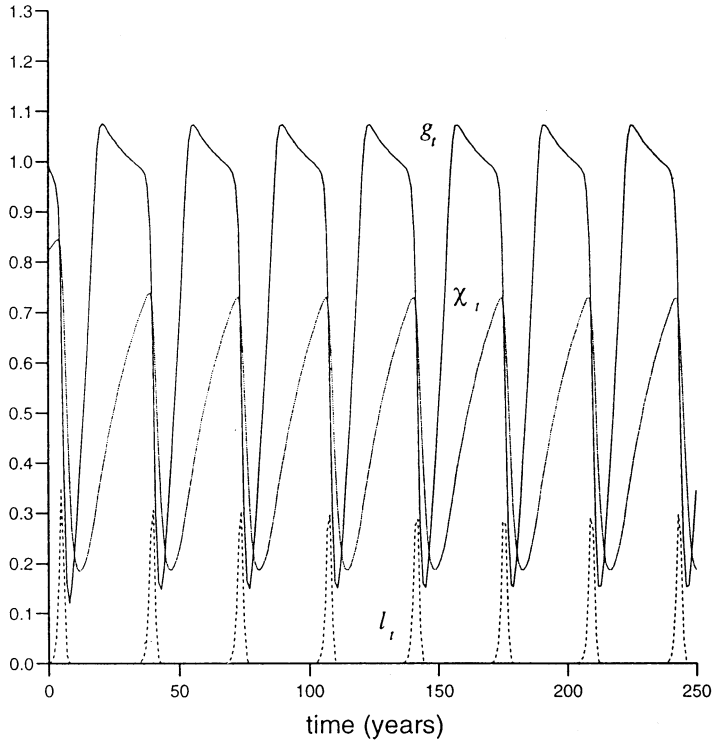

Fig. 13. Periodic outbreaks in a simulation of the three-variable reduced model given by equations (5.5). The period is about 35 years, as indicated by the variation in l (larval density), g (foliage density), and χ (mature tree fraction).

including the regeneration term

$$\gamma = \frac{\lambda_3 \phi}{\sigma(1-\mu V)\chi} \approx \frac{\bar{\gamma}(1-\chi)}{\chi}, \tag{5.7}$$

we use $l_{t+1} - l_t \approx \dot{l}$, etc., to rewrite (4.15) as

$$\begin{aligned} \dot{l} &= \left[\frac{K(v)H(v)\chi}{g} - 1\right] l, \\ \dot{g} &= \frac{\bar{\gamma}(1-\chi)}{\chi} + H(v) - g, \\ \dot{\chi} &= -[1 - m(v)]\chi + \Psi_5(1-\chi), \end{aligned} \tag{5.8}$$

where $v = g\exp(-l/g)$, we take $\phi \approx \Psi_5(1-\chi)$ and also include the source term in χ (see $(3.5)_2$) to regenerate χ following an outbreak. In

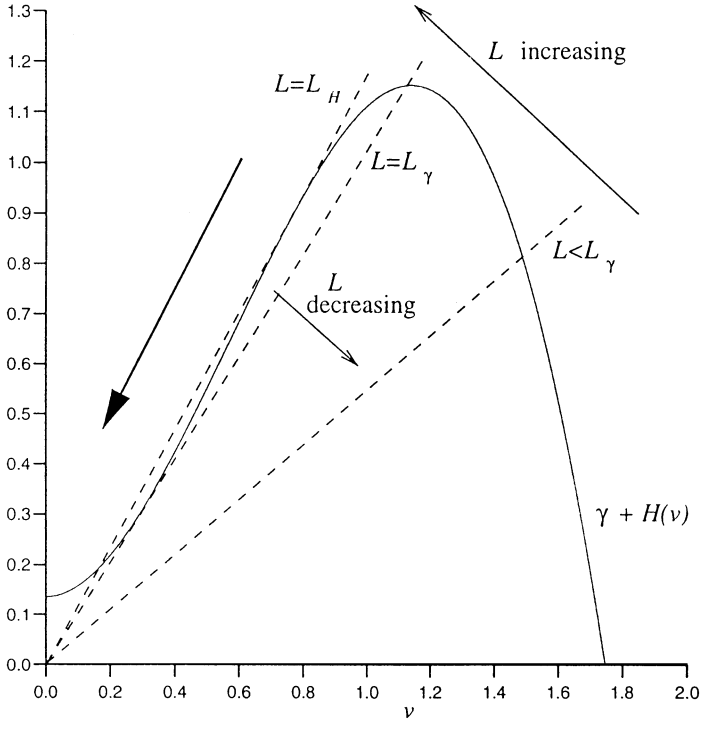

Fig. 14. Modification to $H(v)$ when γ is added. Saddle node bifurcations for v occur at the values $L = L_{\mathrm{H}}$ and $L = L_{\gamma}$.

$(5.8)_{1,2}$ we have replaced χ_{t+1} by χ. One could also justify replacing it by $m(v)\chi$, although the difference would be expected to be minor. In the two-dimensional version we would take χ as constant, and ignore the last equation. These equations are very different from those of the LJH model, even at a mechanistic level, although they both describe the same basic processes. It is thus impressive that the behaviour of the two models is so similar. For comparison, the LJH model (with B, S, E replaced by l, χ, g respectively) is, roughly,

$$\dot{l} = l\left[r_B\left\{1 - \frac{l}{K'}\left(\frac{T_E^2 + g^2}{g^2}\right)\right\} - \frac{\beta l}{\alpha'^2 + l^2}\right],$$

$$\dot{g} = r_E g\left(1 - \frac{g}{K_E}\right) - \frac{P' l g^2}{T_E^2 + g^2},$$

$$\dot{\chi} = r_s \chi\left[1 - \frac{\chi}{g}\frac{K_E}{K_S}\right]. \tag{5.9}$$

In writing (5.9), we have identified B/S (larvae per branch in the LJH model) with l (larvae per ten square feet of branch area), but simply put $\dot{B}/S = \dot{l}$, consistent with the phenomenological tone of the LJH model.

In summary, while both the LJH model and the Jones site model represent the basic mechanisms, they do so in very different ways. Nevertheless, it is possible to reduce the Jones model methodically (in the absence of a detailed age structure) to a skeletal model which bears comparison with the LJH model. While the models at this level are still very different, they both exhibit oscillations due to a similar process of cycling round hysteresis loops, and one would infer that this oscillation mechanism is rather robust to the choice of model used.

We have also examined the effect of including a number of different sites, each following the dynamics of the reduced three variable model, either with collapse (4.15) or with regeneration (5.5). Moth migration is a very important practical consideration. The hatched moths disperse widely via decisive 'exodus flights' from above the forest canopy in the evening, depending on weather conditions (Greenbank et al. 1980), and this effect can be modelled by including a migration term to neighbouring sites. Figure 15 shows a typical result of one such simulation. We have chosen a one-dimensional array of sites for illustrative purposes, and have included migration by allowing a prescribed fraction (ranging from 0.05 to 0.5) to migrate to neighbouring cells. The main effect of migration is initially to cause a wave of outbreaks to propagate along the sites. At larger times, the outbreaks in all sites become synchronised. The continuous analogue of inter-site migration would be the inclusion of a diffusion term for l in (5.9) (Ludwig et al. 1979), and the travelling wave is expected in this case also (Murray 1989). It should be pointed out that the size of the diffusion coefficient would be of $O(\bar{d}^2/\Delta t)$, where $\bar{d}$ is the root mean square distance travelled by a (random walking) moth in a time Δt. If we assume that a female moth lays a half of her egg complement at the natal site, and the other half at distance $\bar{d}$ after one or several migrations, then the appropriate value of Δt is one year, which is the life cycle time. The migration distance can be very large; for the root mean square, if we take $\bar{d}$ to be 10 km, then the diffusion coefficient is 100 $\mathrm{km}^2\,\mathrm{y}^{-1}$, and the diffusion distance over a typical outbreak time of 6 years is 25 km. For comparison, the Jones site model in New Brunswick considered an area roughly 250 km square, with each site being about 13 km square.

For the regenerative model, the typical behaviour as described above is found over a wide range of migration parameters. In addition, if migration is large enough, then the collapse model without regeneration can also lead to a travelling wave of outbreaks, since in the collapse phase of the outbreak, enough moths can migrate to healthy

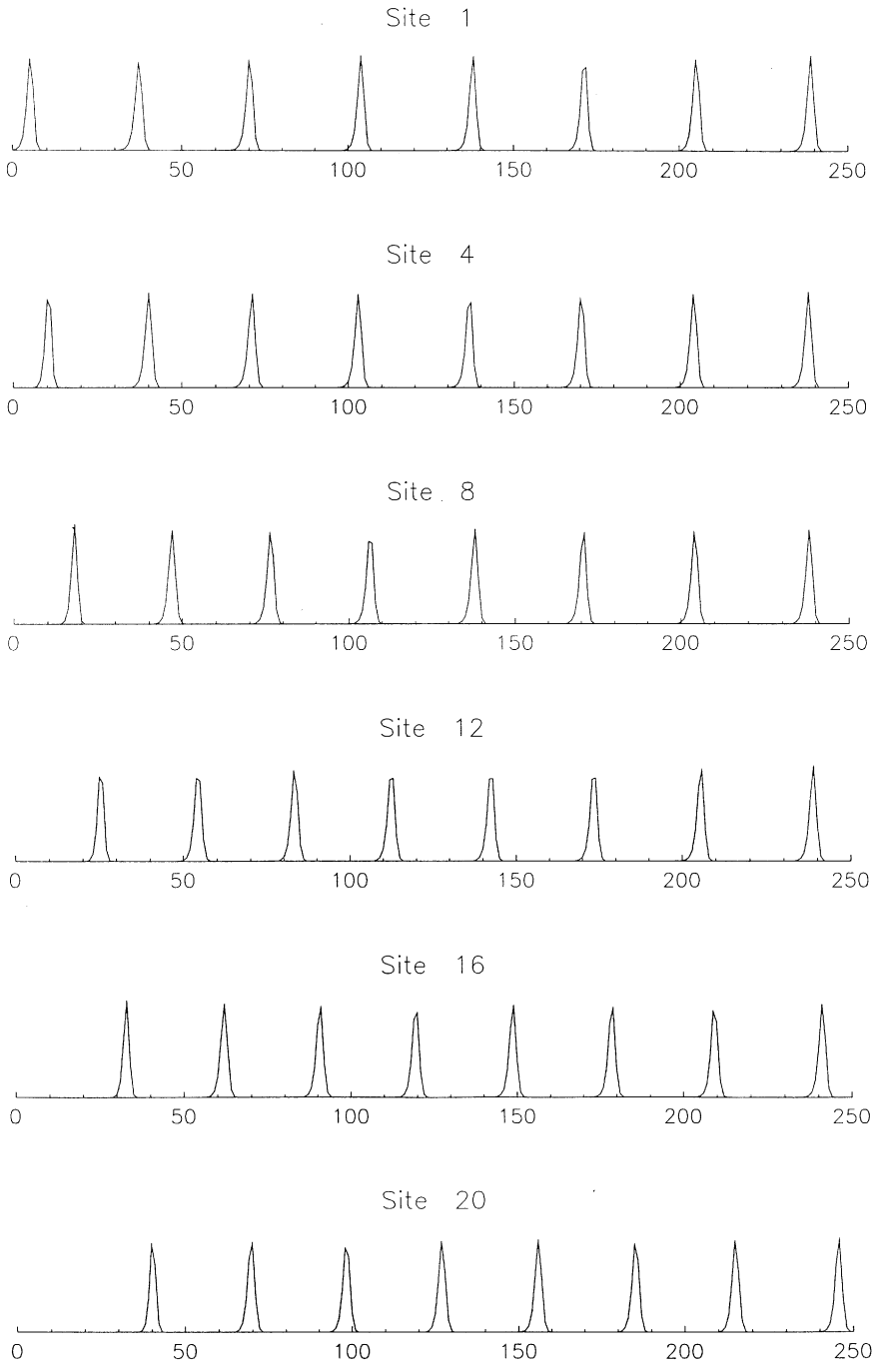

Fig. 15. Sequential oscillations in adjoining sites of the regenerative model (5.5), when a fraction 0.05 migrates to adjoining cells (0.025 to each, except at the end sites). Twenty sites were used, of which we show only six for clarity. The initial outbreaks take the form of a travelling wave, but by about 300 years, these have synchronised to a spatially independent periodic solution.

forest to initiate new outbreaks. On a finite set of sites, however, collapse eventually occurs everywhere.

6. Conclusions

We have shown that the Jones site model can be reduced to a set of two, or three, difference equations, by making two hefty but relatively justifiable assumptions. Firstly, the detailed age structure of the site model is telescoped by defining three tree fractions, namely young, mature and old trees, and then we showed that it is realistic to consider only the mature tree fraction χ. Secondly, although it is an essential part of the budworm lifestyle to consume new (first year) foliage where available, from the point of view of the model, the distinction between new and old foliage appears to be a mathematical detail which is inessential to the mechanism of oscillation.

In discussing this reduced three variable model, it becomes apparent that the tree fraction variable χ is also of secondary interest; the main gist of the model, and the mechanism for oscillation, can be understood by reference to the two variable model, (4.17) and (4.19).

In its most basic form, we can think of (4.19) as providing a year to year difference equation for the foliage variable g, whose evolution is determined by the shape of the unimodal function $H(v)$ portrayed in Fig. 7. The key features of this curve which allow a collapse to occur are its maximum, and the quadratic behaviour at small v. Both of these features follow from the assumption, enunciated before (2.7), that the growth rate W_2 is a parabolic function of photosynthetic assimilation $\bar{A}$, which is itself proportional to foliage density. This is a very reasonable assumption, since the foliage density must saturate at a maximum value on a healthy tree.

The dependence of this evolution from year to year is modulated by the larval density, because the growth of foliage occurs in the summer, while larval defoliation occurs mostly in the winter. Thus really the foliage in September of year $t+1$ (g_{t+1}) is determined not directly by g_t, but by the foliage in spring v_t surviving from consumption by the overwintering larvae. Evidently, the more larvae (l), then the lower v_t will be, and the effect of this in determining g_{t+1} in terms of g_t is to stretch out the graph of H in Fig. 7 as l increases: thus, gradual increase of l will eventually lead to collapse of the foliage via the hysteresis implicit in Fig. 7.

Growth from year to year of the larval population is mediated in a complicated way by the foliage, and in particular the survival through successive instars depends essentially on the spring foliage v_t.

The growth is described by the function $K(v)$ depicted in Fig. 8, thus the larval population declines at small foliage levels, and grows at large ones. This then allows the outbreak-collapse mechanism to operate. At low larval densities, foliage is healthy and resides at the positive steady state of $g = H(v)$. As l increases, the graph of H is pulled to the right, and at a critical value, the equilibrium disappears and the foliage collapses. As a consequence, the larval population begins to collapse.

In principle, the low levels of l could now lead to recovery of the foliage, though this does not actually happen in the two variable model. Instead, recovery occurs in the Jones site model because young trees of age less than about 20 years are resistant to budworm attack. Thus, these trees provide a small but non-zero source of new foliage, which has the effect of raising the foliage growth term from zero when $v = 0$ (see Fig. 14), and this allows a hysteretic switch between healthy and diseased states as larval population varies, and regeneration of the forest following an outbreak.

6.1. Royama's model

Royama (1984, 1992) criticised earlier models of budworm outbreaks for a variety of reasons. He conceptualised these (based on Morris (1963)) as having multiple equilibrium structures, so that outbreaks would be initiated via climatically induced transients from an endemic state to a high budworm outbreak state at isolated centres, and these would spread via migrations.

It is probably dynamically naïve to suppose that cyclic weather patterns could cause strongly periodic oscillations with 35 year periods, as suggested by Wellington et al. (1950) and in fact both the Jones model and the LJH model exhibit self-sustained oscillations. Nor is it essential to the Jones/LJH theories that outbreaks are initiated at epicentres, a notion which Royama also rejects. Royama also states that the existence of a multiple equilibrium structure is not substantiated by data, commenting that this interpretation of the data by Watt (1963) is inadmissible. While the criticism may be valid, it is in fact also inaccurate to associate self-sustained oscillations with multiple *equilibria*, and this in itself may sideline the criticism of Watt's analysis. As described above, the essence of the oscillations above can be described by a hysteretic switching between *quasi-equilibrium* states – not at all the same thing, and these are very robustly described in terms of foliage dynamics. The point is made explicitly in the LJH model where Fowler (1997) shows that there is typically *one* steady state (the intersection of the E curve and S curve

number 2 in Fig. 11.8) in conditions where self-sustained oscillations occur.

Royama's substantive criticisms are then two in number. The first is that food shortage was not a primary universal cause of budworm decline, since decline happens everywhere simultaneously independently of defoliation. The second is that moth invasions only lead to an outbreak phase (in good foliage conditions) if the population overall is growing. Royama quotes the example of a plot (G4) in the Green River area where large moth invasions in 1954, 1957 and 1961 led to temporary increases in larval populations, following which the declining trend continued.

These are serious considerations, but we consider that a plausible remedy is at hand. The effect of moth migration in the model is the inclusion of a dispersal term, which has been described briefly above. It is perhaps easiest to understand in its continuous manifestation, as a diffusion term (although in reality the direction of prevailing winds will make this a severe over-simplification). We mentioned an rms dispersal distance of 10 km, which gives a diffusion distance of 10 km over a year; but dispersals can be of much longer range, and more particularly, by their nature are not really confined locally. A better conceptualisation of migration may be via mixing, and if this is efficient enough, then the budworm population in a large area will essentially respond uniformly to foliage changes; on the other hand, since trees do not migrate, it can be expected that the stochastic nature of migrations and landing patterns will lead to irregular distributions of defoliation and tree mortality. The implication of this is that in assessing the validity of the Jones model, one needs to take spatial averages of foliage and tree density in assessing functional dependence of these on budworm survival and fecundity. We see that from this perspective, Royama's two criticisms are based precisely on not doing this.

Given his rejection of the foliage/budworm interaction theory, Royama proposes that a population model of predator prey type may explain the oscillations. The predators are various classes of parasitic wasp which prey exclusively on the budworm larvae, and are indeed an integral part of the budworm life cycle. It is well known that predator-prey models can indeed oscillate, although Royama offers no specific model. In the absence of such a model, it is difficult to be categorical, but we consider the following observation to make this suggestion less likely. The occurrence of a 35 year oscillation requires a dynamical process operating on this sort of time scale. We have seen that tree regeneration provides exactly this in the Jones model. However, the budworm and its parasites enjoy the same annual time scale, and it is difficult to see how a 35 year period could occur without some other

controlling influence on the dynamics. For example, a stable period 35 orbit for a first order difference equation requires a very particular type of functional map, and its dynamics would in any case be destroyed by noise. We therefore consider that the Jones model remains the best one available.

Appendix: variables and parameters

Listed here are the main variables and parameters of the model along with their definition and units. In reference to Jones' original paper, his notation is given also. Densities of spruce budworm and foliage are denoted almost exclusively by lower case roman letters; the only exceptions being $\bar{v}$, v_0 and v_1 (numbers of eggs). Upper case Greek characters denote constant parameters which are not densities, although some capital roman letters are also used for this purpose.

Quantity	Jones	Description and units (where applicable)
A.1. Large larval update		
l	N_L	large larval density (ind tsf^{-1})
A.2. Small larvae		
S	S_S	proportion of small larvae surviving
I	P_{SS}	probability of two successful small larval searches
G_1	P_1	probability of a successful autumn search
G_2	P_2	probability of a successful spring search
B	SAR	relative branch surface area of susceptible trees after age update
s	N_S	small larval density (ind tsf^{-1})
Θ_0	k_S	constant parameter
A.3. Production of eggs		
E	S_E	proportion of eggs surviving (constant)
e	N_E	egg density (ind tsf^{-1})
$\bar{a}$	e_P	potential egg density (ind tsf^{-1})
d	e_g	egg density generated on site (ind tsf^{-1})
A	S_F	female survival rate (constant)

Λ_3	A_{PF}	constant parameter
Λ_4	B_{PF}	constant parameter
R	P_F	proportion of adults which are female

A.4. Fecundity

M	WGT	the average relative weight of pupae
Σ_0	A_{F1}	constant parameter
Σ_1	A_{F2}	constant parameter
Σ_2	B_F	constant parameter
$\bar{v}$	FEC	number of eggs carried per female
v_0	–	mean lower bound to egg production (number of eggs)
v_1	–	mean upper bound to egg production (number of eggs)

A.5. Pupae

a	N_A	density of adults generated on site (ind tsf^{-1})
P	S_P	survival rate of pupae
Υ_0	A_P	constant parameter
Υ_1	B_P	constant parameter
p	N_P	density of pupae (ind tsf^{-1})

A.6. Large larvae

K	S''_L	survival rate of large larvae to instar VI
Φ_0	k_L	constant scaling factor
$\bar{X}$	S'_L	survival rate from parasitism
W	W_F	the weather factor
k	N_6	density of instar VI larvae (ind tsf^{-1})
$\bar{k}$	$Prey$	effective density of instar VI larvae (ind tsf^{-1})
P_j	$Pred_j$	large larval proportion lost to class j avian predation
C_j	α_j	a class j predation coefficient (constant)
$\bar{P}$	S_{PRED}	net survival rate from predation
Q	$PRED$	total functional response to predation
A_0	AK	'clumping' coefficient of avian predation (constant)
L	S_L	total survival rate of large larvae to pupation

A.7. Large larval feeding

c_0	d_0	maximum total foliage consumption (fu ind^{-1} year^{-1})
q	d_1	actual new foliage consumption (fu ind^{-1} year^{-1})
r	d_2	actual old foliage consumption (fu ind^{-1} year^{-1})
X	$DR1$	relative consumption of new foliage
Y	$DR2$	relative consumption of old foliage
Z	DR	relative consumption of all foliage

A.8. Foliage update

f	F_1	new foliage density at start of year (fu tsf^{-1})
g	F_2	old foliage density at start of year (fu tsf^{-1})
h	F_T	total foliage density at start of year (fu tsf^{-1})
f_0	–	new foliage density with no budworm (constant) (fu tsf^{-1})
g_0	–	old foliage density with no budworm (constant) (fu tsf^{-1})
h_0	–	total foliage density with no budworm (constant) (fu tsf^{-1})

A.9. Budworm defoliation

$\bar{q}$	$DEF1$	density new foliage removed by larvae (fu tsf^{-1})
$\bar{r}$	$DEF2$	density old foliage removed by larvae (fu tsf^{-1})
u	F_1^*	new foliage level after defoliation (fu tsf^{-1})
v	F_2^*	old foliage level after defoliation (fu tsf^{-1})
w	F_T^*	total foliage level after defoliation (fu tsf^{-1})

A.10. Spring foliage production

$\bar{A}$	A	photosynthetic assimilation rate
m	F'_1	new foliage density due to photosynthesis (fu tsf^{-1})
W_1	S_{F_1}	fraction of new foliage surviving tree mortality
W_2	S_{F_2}	fraction of old foliage surviving tree mortality and aging
n	F'_2	density of old foliage carried into the next year (fu tsf^{-1})

A.11. Foliage after mortality

$\bar{x}$	F_1^d	new foliage density on trees to die (fu tsf^{-1})
$\bar{y}$	F_2^d	old foliage density on trees to die (fu tsf^{-1})
Γ_0	δ	constant parameter
x	F_1^{**}	new foliage density after tree mortality (fu tsf^{-1})
y	F_2^{**}	old foliage density after tree mortality (fu tsf^{-1})
z	F_T^{**}	total foliage density after tree mortality (fu tsf^{-1})

A.12. Budworm induced mortality

V	R_{SA}	susceptible branch surface area reduction factor due to budworm
T	S_{BW}	measure of budworm induced tree stress
Ψ_2	S_0	constant parameter
U	F_R	relative old foliage level after defoliation

A.13. Removal of dead trees

M_i	M_i	fraction of trees in age class i dying due to budworm
μ_i	μ_i	age specific budworm susceptibility factor
C	RG_{BW}	fraction host land regenerated after budworm mortality
T_i	T_i	fraction of host land occupied by trees of age class i
D	T_{sp}^*	susceptible host land fraction before mortality and aging
J	R_L	host land fraction of surviving trees
U_i	T_i^*	fraction of land in age class i not succumbing to budworm
Ψ_3	–	natural mortality rate in age clases 74, 75 (constant)
$\bar{H}$	RG_{75}	fraction of host land regenerated after natural death
V_i	T_i^{**}	fraction of class i trees surviving natural mortality ($i = 74, 75$)
b	SA	susceptible branch surface area after tree update (tsf $acre^{-1}$)
σ_i	σ_i	branch surface area of trees in age class i (tsf $acre^{-1}$)

$\bar{C}$	$\overline{T_{21}}$	fraction of host trees becoming susceptible next year
c	SA_{21}	surface area of trees about to become susceptible (tsf acre^{-1})
$\bar{D}$	T_{sp}	proportion of susceptible host land after tree update.

References

Belyea, R. N., C. A. Miller, G. L. Baskerville, E. G. Kettela, K. B. Marshall and I. W. Varty 1975 The spruce budworm. (A series of eight articles.) Forestry Chronicle **51**, 135–160

Fowler, A. C. (1997) Mathematical models in the applied sciences. CUP, Cambridge

Greenbank, D. O., G. W. Schaefer and R. C. Rainey (1980) Spruce budworm (Lepidoptera: Tortricidae) moth flight and dispersal: new understanding from canopy observations, radar and aircraft. Entomological Society of Canada Memoir, Vol. 110

Griffiths, K. J. and C. S. Holling (1969) A competition submodel for parasites and predators. Canad. Entomol. **101**, 785–818

Horowitz, I. and A. Ioinovici (1985) Budworm-forest system: application of quantitative feedback theory. Int. J. Syst. Sci. **16**, 209–225

Jones, D. D. (1979) The budworm site model. In: Norton, C. A. and C. S. Holling, eds.: Pest management, proceedings of an international conference, October 25–29, 1976, Pergamon Press, Oxford, pp. 91–155

Ludwig, D., D. G. Aronson and H. F. Weinberger (1979) Spatial patterning of the spruce budworm. J. Math. Biol. **8**, 217–238

Ludwig, D., D. D. Jones and C. S. Holling (1978) Qualitative analysis of insect outbreak systems: the spruce budworm and forest. J. Anim. Ecol. **47**, 315–332

May, R. M. (1978) Host-parasitoid systems in patchy environments, a phenomenonological model. J. Anim. Ecol. **47**, 833–843

McNamee, P. J., J. M. McLeod and C. S. Holling (1981) The structure and behaviour of defoliating insect/forest systems. Res. Popul. Ecol. **23**, 280–298

Mook, L. J. (1963) Birds and the spruce budworm. In: Morris (1963), pp. 268–271

Morris, R. F. (ed.) (1963) The dynamics of epidemic spruce budworm populations. Entomological Society of Canada Memoir, Vol. 31 (332 pages)

Murray, J. D. (1989) Mathematical biology. Springer-Verlag, Berlin

Régnière, J. and M. You (1991) A simulation model of spruce budworm (Lepidoptera: Tortricidae) feeding on balsam fir and white spruce. Ecol. Modell. **54**, 277–298

Royama, T. (1984) Population dynamics of the spruce budworm *Choristoneura fumiferana*. Ecol. Monogr. **54**, 429–462

Royama, T. (1992) Analytical population dynamics. Chapman and Hall, London

Stedinger, J. R. (1984) A spruce budworm-forest model and its implications for suppression programs. Forest. Sci. **30**, 597–615

Watt, K. E. F. (1963) The analysis of the survival of large larvae in the unsprayed area. In Morris, R. F. (ed.) The dynamics of epidemic spruce budworm populations. Entomological Society of Canada Memoir, Vol. 31, pp. 52–63

Wellington, W. G., J. J. Fettes, K. B. Turner and R. M. Belyea (1950) Physical and biological indicators of the development of outbreaks of the spruce budworm. Canad. J. Res. D**28**, 303–331